J. Physiol. (1987), **385**, *pp.* 325–359
With 12 text-figures
Printed in Great Britain

ACTIVATION OF ACETYLCHOLINE RECEPTORS ON CLONAL MAMMALIAN BC3H–1 CELLS BY HIGH CONCENTRATIONS OF AGONIST

BY STEVEN M. SINE* AND JOE HENRY STEINBACH†

From the Salk Institute, P.O. Box 85800, San Diego, CA 92138, U.S.A. and the †Department of Anesthesiology, Washington University School of Medicine, 660 South Euclid Avenue, St Louis, MO 63110, U.S.A.

(*Received 14 April 1986*)

SUMMARY

1. Currents were recorded through acetylcholine (ACh) receptor channels on clonal BC3H–1 cells in the presence of high concentrations of ACh (20–1000 μM) and carbamylcholine (180–1000 μM).

2. Channel openings at high agonist concentrations occur in clusters separated by long silent periods (seconds). Clusters, in turn, show groups of closely spaced openings separated by relatively long (hundreds of milliseconds) closed periods. The closed periods between clusters and between groups within clusters are thought to reflect two desensitized states (Sakmann, Patlak & Neher, 1980).

3. Openings within groups consist largely of long-duration openings. An excess of brief-duration openings is seen at all high agonist concentrations; most brief openings occur as isolated, solitary openings.

4. The distribution of closed periods within groups shows four exponential components with time constants separated by several fold over the range of 50 μs to 50 ms.

5. The distribution of closed periods within groups is analysed as a function of agonist concentration, to estimate rate constants for transitions in a hypothetical reaction scheme for receptor activation. One or two of these components (depending on agonist and agonist concentration) appear to reflect agonist binding and channel gating. It is hypothesized that the other closed-period components within groups at high agonist concentrations result from additional states of doubly liganded receptors which have closed ion channels.

6. With ACh as agonist the data indicate that binding and activation saturate at concentrations above 130 μM. The data are quantitatively consistent with measurements made at low concentrations of ACh (Sine & Steinbach, 1986*b*), and indicate that a four-state linear scheme is able to describe major features of ACh-receptor activation on BC3H–1 cells. The channel opening rate is estimated to be about 450 s^{-1} and the closing rate about 35 s^{-1} (−70 mV, 11 °C). The concentration

* Present address: Department of Physiology, Yale University School of Medicine, New Haven, CT 06510, U.S.A.

† Author and address for correspondence.

dependence of closed durations suggests that some positive co-operativity exists in agonist binding. The dissociation constant with one ACh molecule bound is about 50 μM, and that with two bound is about 10 μM (for an ACh receptor with a closed channel).

7. Saturation is not observed with carbamylcholine, even at 1 mM. The data are consistent with data obtained at low concentrations of carbamylcholine, and are in over-all agreement with the interpretation of data obtained with ACh. The affinity for carbamylcholine is estimated to be about 20-fold lower than with ACh.

8. Clusters of openings appear to arise from a largely homogeneous population of receptors. However, the mean open time differs significantly from one cluster to another in most patches. The mean open times for clusters in a given patch appear to be normally distributed. These observations suggest that individual ACh receptors differ in some functional properties, but apparently are drawn from a single normally distributed population.

INTRODUCTION

A preceding paper analyses the kinetic properties of currents through single acetylcholine-receptor (AChR) channels elicited by low concentrations of agonist (Sine & Steinbach, 1986*b*). The low-concentration experiments support a sequential scheme for receptor activation in which the agonist binds to the receptor and induces relatively slow conformational changes that open and close the receptor channel. The data were analysed to give estimates of three rate constants within the sequential scheme: the channel opening rate (β), the channel closing rate (α), and the agonist dissociation rate (k_{-2}). β and k_{-2} are comparable in magnitude, so that on average the channel opens and closes several times once the receptor channel opens. β is also much larger than α such that the doubly occupied receptor has a high probability of being open ($\beta/(\beta+\alpha) = 0{\cdot}93$ for ACh). These aspects of receptor activation may be explored further by experiments in which single-channel currents are activated by high concentrations of agonist.

Under the influence of high agonist concentration, single-channel currents appear as groups, or sudden episodes of many channel openings interrupted by brief closed periods (Sakmann *et al.* 1980; Sine & Steinbach, 1984*a*). At sufficiently high concentrations, these brief interruptions are predicted to decay with the rate β, the opening rate of the doubly occupied receptor (Colquhoun & Hawkes, 1981). In addition, the probability of channel opening may be measured directly as the fraction of time the channel spends in the open state within a group of openings. Therefore, measurements acquired at high agonist concentrations complement the low-concentration measurements by providing independent estimates of both the channel opening rate and the opening probability.

The present experiments use the patch-clamp technique to examine the activation of AChR channels induced by high concentrations of ACh and carbamylcholine. For both agonists, a major closed-duration component is identified whose mean duration approaches the value of β estimated from the low-concentration measurements. Furthermore, at non-saturating agonist concentrations a second major brief closed-duration component is observed which is interpreted as resulting from agonist

association and dissociation steps as well as channel opening. The concentration dependence of the closed durations suggests that agonist binding exhibits positive co-operativity.

METHODS

The present high-agonist-concentration experiments were conducted in parallel with the companion low-concentration experiments (Sine & Steinbach, 1986*b*). Essentially identical conditions were used in both sets of experiments. Several key experimental conditions were maintained in the present high-concentration work. BC3H-1 cells were grown under differentiating conditions (0·5 % cadet calf serum), protease treated on days 4 or 5 (collagenase followed by pancreatin), and examined for agonist-induced single-channel currents 4–6 days later. Currents were recorded using the 'cell-attached' patch configuration at a temperature, T, of 11 °C and an applied potential, V, of +70 mV (relative to the cell interior). The following extracellular solution was used: 140 mM-KCl, 5·4 mM-NaCl, 1·8 mM-$CaCl_2$, 1·7 mM-$MgCl_2$, 25 mM-HEPES, adjusted to pH 7·4 with 10 mM-NaOH. In this high-K^+ solution the resting potential of the cells is 0 mV, so the potential across the patch of membrane is −70 mV (inside minus pipette). The pipette solution consisted of: 142 mM-KCl, 5·4 mM-NaCl, 1·8 mM-$CaCl_2$, 1·7 mM-$MgCl_2$, 9·5 mM-HEPES, adjusted to pH 7·4 with 5 mM-NaOH.

Single-channel currents were recorded on FM analog tape (15 in s^{-1}, Racal Store 4DS) and replayed for later analysis. Currents were filtered at 7200 Hz (low-pass Bessel, −3 dB point) and periods of channel activity were sampled at 25 μs intervals using an interrupt-driven sampling program (provided by Dr F. J. Sigworth). Channel-opening and channel-closing transitions were detected using a threshold-crossing procedure with the detection threshold set at one-half the mean open-channel current. Open- and closed-duration histograms were constructed for events exceeding a specified dead time (100 μs) and were fitted by the sum of exponentials as described previously (Sine & Steinbach, 1986*a*, *b*). The rate of occurrence for a given closed-duration component was calculated from the total area of a fitted component (corrected for limited resolution) divided by the total open time for the experiment.

RESULTS

Qualitative features of currents induced by high ACh concentrations

Fig. 1 shows the qualitative features of single-channel currents induced by 130 μM-ACh, a near-saturating agonist concentration (see following sections). Channel openings appear as episodes of intense activity, termed clusters, separated by prolonged quiescent periods lasting several seconds. Clusters, in turn, consist of several groups of more closely spaced active periods separated by closures lasting several hundreds of milliseconds. Closed periods between clusters reflect the recovery rate of the population of receptors from the slowly recovering desensitized state, whereas closures between groups reflect the recovery rate of a single receptor from the rapidly recovering desensitized state (Sakmann *et al.* 1980). A group of openings is illustrated at high temporal resolution in the lower four traces of Fig. 1. Within the group, the current switches between discrete levels, reflecting either open or closed receptor states. In addition to the appearance of groups and clusters, infrequent solitary openings are observed, belonging primarily to the short-duration-opening population. In the present paper, attention is turned to the fast kinetic processes occurring within groups of channel openings.

Summary of low-concentration-agonist predictions

Single-channel recordings at low ACh concentrations reveal two distinct classes of short-duration closures: brief (mean duration, 50 μs) and intermediate duration (mean, 0·5–1 ms; Sine & Steinbach, 1986*b*). For three strong agonists (ACh, carba-

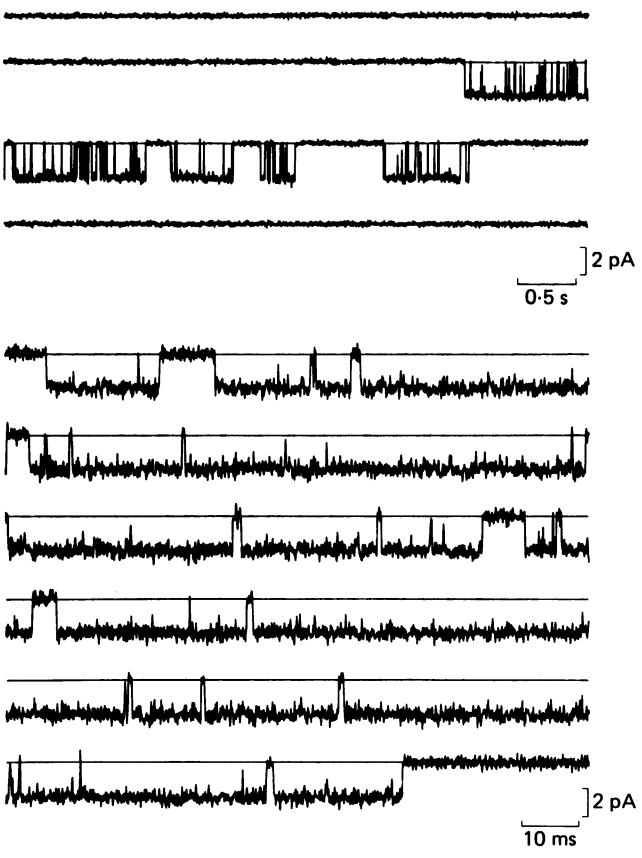

Fig. 1. Single-channel currents induced by 130 μM-ACh. Top four traces: a single cluster of channel openings containing five apparent groups and four intergroup intervals (low-pass filtered at 1000 Hz; each trace 5 s long). Bottom five traces: openings within a single group from the cluster shown above (low-pass filtered at 4000 Hz, each trace 102·4 ms long). The continuous lines indicate the mean base-line current. Currents were recorded from a cell-attached patch with high-potassium–normal-calcium solution in both the bath and the recording pipette. $V = -70$ mV and $T = 11$ °C.

mylcholine and suberyldicholine), intermediate-duration closures show agonist specificity in both their time constant and frequency of occurrence. Brief-duration closures, in contrast, display essentially identical properties for all three agonists. Scheme (1) is consistent with the two types of closures seen at low agonist concentrations:

$$A + R \underset{k_{-1}}{\overset{k_1[A]}{\rightleftharpoons}} AR \underset{k_{-2}}{\overset{k_2[A]}{\rightleftharpoons}} A_2R \underset{\alpha}{\overset{\beta}{\rightleftharpoons}} A_2R^* \underset{b}{\overset{f}{\rightleftharpoons}} A_2R'. \qquad \text{scheme (1)}$$

In scheme 1, two agonists (A) associate with the receptor (R) with forward rate constants, k_1 and k_2, and dissociate with rate constants k_{-1} and k_{-2}. The doubly occupied receptor (A_2R) adopts the open state (A_2R^*) with rate constant β, and the open state dissipates to A_2R with rate constant α. A_2R' is a short-duration closed state which is intrinsic to the open channel, *per se*, with transition rate constants

between A_2R^* and A_2R' of f and b. Due to their agonist specificity, intermediate-duration closures are suggested to represent dwells in A_2R. Brief closures, then, correspond to dwells in A_2R'. Analysis of intermediate closures with ACh as agonist yields a channel opening rate estimate, β, of 400–500 s^{-1}, and a closing rate, α, of 35 s^{-1} (−70 mV, 11 °C; Sine & Steinbach, 1986*b*). The following section examines closures within groups at a saturating ACh concentration in order to independently estimate β and α.

Analysis of closed durations in the presence of high agonist concentrations

Fig. 2 shows the distribution of closed durations obtained from one patch in the presence of 1 mM-ACh, a concentration well above the apparent dissociation constant (3–30 μM, Cash, Aoshima & Hess, 1981) and the highest concentration used in these experiments. The closed-duration histogram is described by the sum of six well-separated exponentials; two long-duration components (termed c_0 and c_1), apparently due to fast and slow desensitization recovery processes, and four short-duration components (termed c_2–c_5), potentially reflecting receptor activation processes. Thus, even first inspection reveals more short-duration components than scheme (1) predicts for a saturating ACh concentration. It seems reasonable, however, that scheme (1) could account for two of the four observed components, whereas the remaining components may result from additional processes separate from those predicted by scheme (1). Therefore, the remainder of the paper attempts to identify the closed-duration components most consistent with a simple receptor activation scheme such as scheme (1).

Two quantities are considered in order to identify the closed dwells associated with the receptor activation steps described by scheme (1). First, at a saturating agonist concentration, the closed-duration component reflecting the A_2R to A_2R^* transition should have a decay rate predicted by the low-concentration estimate of β. Secondly, the frequency of occurrence (the total number of closures in the fitted component divided by the total open time) of these activation-related closures should be close to α, the channel closing rate, also measured at low agonist concentrations. Therefore, in the presence of 1 mM-ACh, we are looking for a closed-duration component with a decay rate of 400–500 s^{-1}, and an occurrence frequency of about 35 s^{-1}.

In the presence of 1 mM-ACh, a major closed-duration component shows a decay rate close to the low-concentration estimate of β (c_3 component in Fig. 2 and Table 1; for three experiments, the decay rate is 465 ± 30 s^{-1}; mean ± S.D.). Closures of the c_3 component occur at a rate of $31{\cdot}5 \pm 9{\cdot}6$ per second of open time, a rate close to the low-concentration α estimate of 35 s^{-1}. The c_3 component, therefore, is a candidate for the closed dwells arising from the A_2R to A_2R^* transition.

The c_5 component has a decay rate of 33000 s^{-1} and an occurrence rate of 250 s^{-1}. About half of the c_5 closures are probably the agonist-independent 50 μs closures (A_2R') seen at lower agonist concentrations (0·1–130 μM; see Table 1 and Sine & Steinbach, 1986*b*). Studies of channel block indicate that about 40 % of the c_5 closures result from fast blockages by ACh (see below and Sine & Steinbach, 1984*b*). The properties of c_5 closures clearly do not match those predicted for the A_2R to A_2R^* transition obtained by analysis of the low-concentration intermediate-duration closures. The c_5 decay rate is also much greater than the value of 12000 s^{-1} predicted

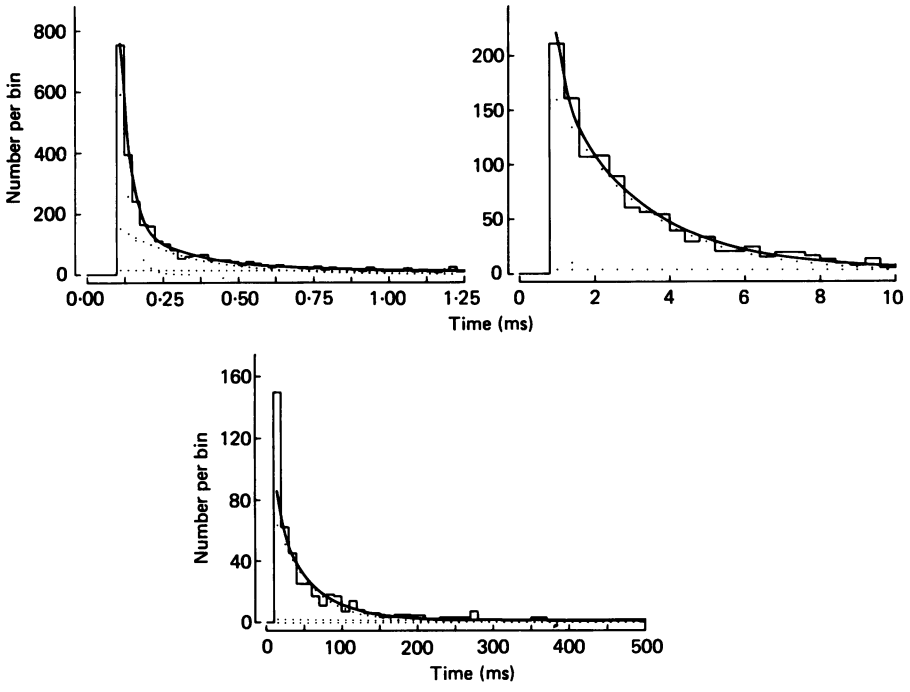

Fig. 2. Closed-duration histogram of currents elicited by 1 mM-ACh at $V = -70$ mV and $T = 11$ °C. The histogram is shown on three time-scales to illustrate the four brief-duration components, c_2–c_5, occurring within groups of openings. The bin size for each panel is, from left to right, 0·025, 0·4 and 10 ms. The histogram is fitted by the sum of six separate exponentials, shown by the uppermost continuous curve, and the contributions of each component by the lower dotted curves. The over-all fit consists of six components, c_0–c_5, with decay rates, l_0–l_5, and total number of events, n_0–n_5: $l_0 = 0{\cdot}177\ s^{-1}$, $n_0 = 78$; $l_1 = 1{\cdot}91\ s^{-1}$, $n_1 = 113$; $l_2 = 22{\cdot}2\ s^{-1}$, $n_2 = 401$; $l_3 = 431\ s^{-1}$, $n_3 = 1420$; $l_4 = 4337\ s^{-1}$, $n_4 = 2136$; $l_5 = 33262\ s^{-1}$, $n_5 = 18694$. Currents were filtered at 7200 Hz and sampled at 25 μs intervals. A total of 4487 events were detected with one multiple opening and a record length of 642 s. The two slowest components, c_0 and c_1, are seen only as flat dotted lines with negligible amplitude in these histograms, although their contribution is included in the over-all sum (continuous curve). The upper left panel is dominated by c_4 and c_5, the upper right panel by c_3 and the lower panel by c_2.

for β even if the low-concentration 50 μs closures were thought to represent dwells in A_2R, although the interference of fast-channel block at 1 mM-ACh could obscure such a 12000 s^{-1} component. The c_5 closures, then, appear to be due to both dwells in A_2R' and fast blockages by ACh.

The c_4 closures show a decay rate of 3700 s^{-1} and occur at a rate of $37{\cdot}2 \pm 9{\cdot}1$ per second of open time. Although the c_4 occurrence rate is close to the α estimated at low concentration, the c_4 decay rate is 10-fold greater than the β predicted from the low-concentration intermediate-duration closures. The c_4 decay rate is also smaller than the value of β estimated if the low-concentration 50 μs closures were considered dwells in A_2R.

The c_2 closures exhibit a decay rate of about 40 s^{-1} and occur at a rate of 13 per second of open time. Again, neither of these properties are consistent with the low-concentration estimates of β and α.

The 1 mM-ACh measurements are consistent with two features of the low-concentration measurements: c_3 closures represent dwells in A_2R and the c_5 closures dwells in A_2R' (and also fast blockage by ACh). The c_2 and c_4 components may represent additional closed states branching from scheme (1).

Estimate of the channel closing rate, α

The true channel closing rate could be calculated if all transitions from A_2R^* to A_2R could be unambiguously identified, which is not possible at present. Inspection of Table 1 indicates that the sum of the rates of occurrence of all closures within groups (c_2–c_5) is far greater than α, estimated at low concentration. If our interpretation of the data is correct, most of the c_2, c_4 and c_5 closures arise from the open state and return directly to the open state. This direct interconnexion is expected for the c_5 closures, whether they arise by channel block or 'flicker'. We have estimated α at high concentration from the sum of the numbers of c_0, c_1 and c_3 closures divided by the total open time (at 1 mM-ACh this gives an estimate of $34{\cdot}8 \pm 6{\cdot}5$ s^{-1}). This procedure is equivalent to assuming that c_0 and c_1 closures (reflecting desensitization) occur largely from A_2R.

The high-concentration α estimate neglects the influence of fast channel block on the apparent open time. Fast block would increase the apparent open time because most blockages would not be resolved, but would appear as high-frequency open-channel noise. The apparent open time, then, would be over-estimated depending on the degree of channel block. At -70 mV, the blocking dissociation constant, K_D, is 5 mM. Therefore, in the presence of 1 mM-ACh the mean open time will be increased by 19%. However, no systematic concentration dependence was observed in the apparent open time, suggesting that the influence of fast block is smaller than the variability from patch to patch.

Estimate of the channel opening probability

At a saturating concentration of agonist, scheme (1) predicts that a receptor will remain doubly liganded and oscillate between states A_2R and A_2R^* (neglecting A_2R'). The fraction of the total time spent in A_2R^* (P_o), therefore, would be $\beta/(\beta+\alpha)$. Experimentally, the fraction of time spent open in a group can be measured by defining a group as a series of openings separated by closed periods of less than 10 ms (at 1 mM-ACh), a time chosen to be about four times the mean duration of the c_3 component. This estimate will be lower than the true probability of being open within a group, as the data show closed-time components within groups in addition to the one ascribed to dwells in A_2R (see above). However, it may also over-estimate the probability of being open, since groups may contain 'hidden' dwells in A_2R preceding the first opening and following the last closing recognized as being within the group, depending on which long-lived closed states arise from or return to A_2R. This over-estimate would be increased if groups contained relatively few openings. As described below, however, (see Fig. 10) most groups contained four or more openings and the mean open time is longer than the mean durations for the c_3–c_5-component closures. The measured fractional open time within groups at 1 mM-ACh is $0{\cdot}912 \pm 0{\cdot}03$ ($n = 3$). An alternative estimate is to calculate the ratio $\beta'/(\beta'+\alpha)$, using the decay rate of the c_3 component as an estimate for β' and $\alpha = 35$ s^{-1}. This gives an estimate for P_o of 0·92.

Summary of results obtained with 1 mM-ACh

The results obtained with saturating ACh concentrations may be summarized as follows. A major closed-duration component, c_3, is seen which apparently reflects the A_2R to A_2R^* transition (see scheme (1)). This assignment is supported by the observations that the c_3 component has a mean duration close to $1/\beta$, and occurs at a rate close to α estimated from the low-concentration measurements. This assignment also results in calculated and measured P_o estimates which are close to those predicted from the low-concentration data. It is emphasized that this interpretation rests on the analysis of one of the four observed brief closed-duration components. The remaining three high-concentration components are less likely candidates for the channel-opening transition because they are not consistent with estimates of α and β from the low-concentration measurements. The following section further explores the identity of the channel-opening transition by examining its concentration dependence.

Concentration dependence of closed durations

Before presenting the experimental concentration dependence of closed durations, the scheme (1) predictions are considered for one set of transition rates which were ultimately found to be consistent with the over-all data. Neglecting the agonist-independent state A_2R' as before, scheme 1 predicts that the probability density function of closed durations, $p(t)$, is the sum of three exponentials:

$$p(t) = Q_0 \lambda_0 e^{-\lambda_0 t} + Q_1 \lambda_1 e^{-\lambda_1 t} + Q_2 \lambda_2 e^{-\lambda_2 t}. \qquad \text{equation (1)}$$

The areas (Q_0, Q_1 and Q_2) and decay rates (λ_0, λ_1 and λ_2) describe the individual time-dependent components, and are defined by the agonist concentration and the rate constants in scheme (1) (k_1, k_{-1}, k_2, k_{-2} and β; see Colquhoun & Hawkes, 1981). Fig. 3 illustrates the predictions of scheme (1), showing the concentration dependencies of the areas and the decay rates for the set of transition rates which will be shown to be appropriate to the data (see Table 2). At limiting low agonist concentrations, two components are predicted, with areas $Q_0 = 0{\cdot}67$ and $Q_2 = 0{\cdot}32$. The decay rate of the larger component, λ_0, describes the opening rate of separate channels, or the rate of leaving the compound closed state ($R + AR + A_2R$). The decay rate of the smaller component, λ_2, describes the reopening rate of one channel, ($\beta + k_{-2}$), or the time dependence of A_2R. A third component, λ_1, is predicted, due to the compound closed state ($AR + A_2R$), but would not be detected at low concentrations because its area approaches zero. At intermediate agonist concentrations (e.g. 20 μM), the area Q_2 approaches zero, yet two components are predicted, with areas $Q_0 = 0{\cdot}47$ and $Q_1 = 0{\cdot}49$, and decay rates $\lambda_0 = 96\ s^{-1}$ and $\lambda_1 = 570\ s^{-1}$. The rate λ_0 corresponds to the effective opening rate of one channel, which we refer to as β'. The decay rate λ_1 gives an estimate of the dissociation rate k_{-1}, as long as the agonist concentration is relatively low. The near-equal areas, Q_0 and Q_1 indicate that a receptor is about equally likely to bind agonist and open from AR as it is to lose its bound agonist at 20 μM-ACh. At concentrations higher than 20 μM, Q_0 increases as Q_1 decreases. Only one component is apparent with decay rate λ_0; λ_0 increases with agonist concentration, approaching the limiting value, β. At saturating concentra-

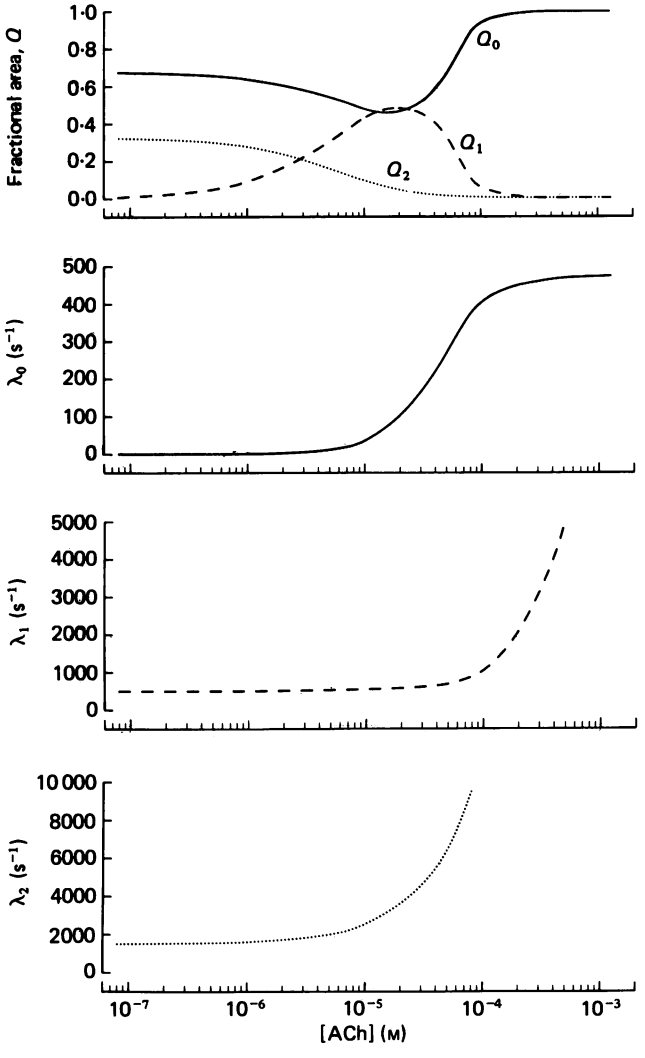

Fig. 3. Predicted concentration dependence of closed dwell times for scheme (1). Top panel shows the fractional areas for the three predicted closed-time components Q_0, Q_1 and Q_2. Three lower panels show the predicted decay rates for the three components, λ_0, λ_1 and λ_2. For each agonist concentration, the decay rates and areas were calculated as follows. The three decay rates are solutions to the cubic equation, $\lambda^3 - b\,\lambda^2 + c\,\lambda - d = 0$, where the coefficients (b, c and d) are defined by the scheme (1) rate constants (k_1, k_{-1}, k_2, k_{-2} and β) and the agonist concentration (see eqns. 3.65–3.67 in Colquhoun & Hawkes (1981)). The three solutions to the cubic equation, λ_0, λ_1 and λ_2, were computed numerically to an accuracy of 0·1 %. The fractional areas were then calculated from eqn. 3.75 in Colquhoun & Hawkes (1981), which is analogous to the text equation for $p(t)$. To convert the fractional area (Q, top panel) to closures per second open time, the ordinal scale should be multiplied by α (the channel closing rate). The parameters used are: $k_1 = 1 \times 10^7$ M^{-1} s^{-1}, $k_{-1} = 500$ s^{-1}, $k_2 = 1 \times 10^8$ M^{-1} s^{-1}, $k_{-2} = 1000$ s^{-1} and $\beta = 480$ s^{-1}.

tions the limiting decay rate reflects the time dependence of the A_2R state. Therefore, over the concentration range examined below (20 μM- to 1 mM-ACh) scheme (1) predicts two major closed-duration components at 20 μM-ACh, and one apparent concentration-dependent component at higher concentrations.

Closed-duration histograms were analysed from recordings made in the presence of ACh concentrations between 20 μM and 1 mM. Representative histograms are shown in Figs. 2 and 4. At these concentrations, four short-duration components are observed, along with two long-duration components due to fast and slow desensitization processes. Our first objective is to identify a concentration-dependent component whose decay rate increases with agonist concentration and reaches a limiting value at saturating concentrations. Secondly, at intermediate agonist concentrations an additional activation component may be resolved, depending on the rates k_{-1} and k_{+2}[ACh]. Finally, the rate of occurrence of closures of these activation components should approach α, the channel closing rate estimated at low agonist concentrations.

The closed-duration histogram analysis is summarized in Table 1. At 20 μM-ACh, the four short-duration components are qualitatively similar, but quantitatively distinct from those observed with 1 mM-ACh: the c_2 decay rate at 20 μM is about twice the corresponding value at 1 mM-ACh, and the 20 μM c_2 closures occur with twice the frequency of c_2 closures at 1 mM. The c_3 decay rate at 20 μM is greater than the corresponding rate at 1 mM, while the 20 μM c_3 closures occur at about half the frequency of the 1 mM c_3 closures. We make the following interpretation of the c_2 and c_3 closures seen at 20 μM- and 1 mM-ACh. At 20 μM-ACh both the c_2 and c_3 components reflect receptor activation steps, whereas at 1 mM-ACh only the c_3 component reflects activation. With 20 μM-ACh, the c_2 component reflects periods in which both bound agonist molecules are lost, and the decay rate for this component gives β' (the 'effective one-channel opening rate'), identified with the λ_0 component in Fig. 3. The c_3 component has a decay rate identified with λ_1 in Fig. 3, which is close to k_{-1} at this concentration. As predicted, the combined c_2 and c_3 occurrence rate closely matches the channel closing rate, α. We have already discussed the reasons why the c_2 closures seen at 1 mM-ACh (decay rate of ~ 50 s^{-1}) represent a process distinct from receptor activation. It is possible, then, that these closures, which are well resolved at 1 mM-ACh, are also present at 20 μM, but are obscured by the more frequent activation-related closures. The presence of such unresolved 50 s^{-1} closures would cause an underestimate of the true β' decay rate, and give an apparently greater occurrence rate.

At 60 μM-ACh, the four short-duration components are similar to those seen with 1 mM-ACh. Inspection of Table 1 shows that the c_3 decay rate is consistently lower than the 1 mM c_3 decay rate. The c_3 occurrence rate at 60 μM is about equal to the 1 mM c_3 occurrence rate, again approaching the low-concentration α estimate. The 60 μM c_3 closures, then, are interpreted as activation-related closed periods with a decay rate, β', approaching the limiting value of β achieved at saturating concentrations.

A second activation component is predicted at 60 μM-ACh (the λ_1 component in Fig. 3). The predicted decay rate is 732 s^{-1}, but the area is predicted to be only one-third the area of the major activation component. Such a second activation

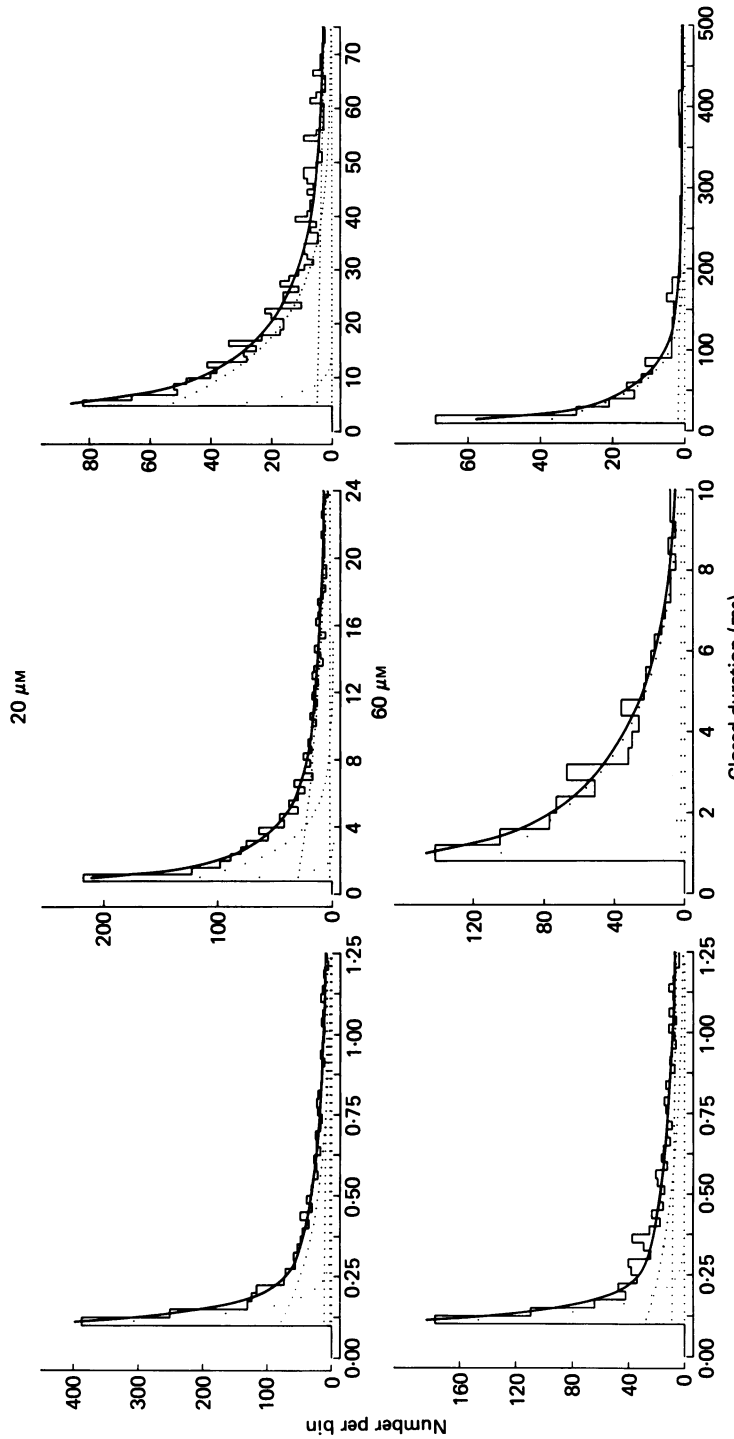

Fig. 4. Closed-duration histograms for currents elicited by 20 μM- (top three panels) and 60 μM-ACh (bottom three panels) at $V = -70$ mV and $T = 11$ °C. Bin sizes: top row, left to right, 0·025, 0·4 and 1·0 ms; bottom row: 0·025, 0·4 and 10 ms. For each ACh concentration, the histogram is fitted by the sum of six separate exponentials. The over-all fit is shown by the upper continuous curve, while the lower dotted curves indicate the contribution of each component. For both concentrations, the over-all fit consists of components, c_0–c_5, with decay rates, l_0–l_5, and the number of events, n_0–n_5. 20 μM: $l_0 = 0{\cdot}479\ s^{-1}$, $n_0 = 97$; $l_1 = 10{\cdot}9\ s^{-1}$, $n_1 = 491$; $l_2 = 79{\cdot}9\ s^{-1}$, $n_2 = 1016$; $l_3 = 522\ s^{-1}$, $n_3 = 926$; $l_4 = 3436\ s^{-1}$, $n_4 = 1283$; $l_5 = 24\,900\ s^{-1}$, $n_5 = 5744$. Total events detected = 4065, three multiple events, and a record length of 1263 s. 60 μM: $l_0 = 0{\cdot}265\ s^{-1}$, $n_0 = 38$; $l_1 = 1{\cdot}93\ s^{-1}$, $n_1 = 97$; $l_2 = 25{\cdot}8\ s^{-1}$, $n_2 = 209$; $l_3 = 392\ s^{-1}$, $n_3 = 982$; $l_4 = 2741\ s^{-1}$, $n_4 = 520$; $l_5 = 24\,515\ s^{-1}$, $n_5 = 2693$. Total events detected = 2009, thirteen multiple events, and the record length was 212 s. Note the prominent components on both middle panels which are postulated to correspond to closed dwells due to receptor activation processes (see Scheme (1) and text).

TABLE 1. Properties of brief closures for ACh

		c_2		c_3		c_4		c_5	
[ACh] (μM)	n	l_2	ν_2	l_3	ν_3	l_4	ν_4	l_5	ν_5
20	2	83·6	21·5	745	15·1	4258	23·8	24903	119
		±5·2	±1·3	±317	±5·9	±1156	±4·1		
60	4	49·3	10·6	342	33·7	3087	17·1	22881	92·3
		±27·1	±7·1	±55·4	±6·6	±1597	±8·8	±1497	±31·7
130	3	55·6	13·9	461	31·5	2338	29·4	27451	125
		±8·2	±4·8	±52·6	±5·0	±287	±3·1	±907	±117
300	2	31·4	17·4	490	34·1	4571	40·9	29264	121
		±23·7	±8·8	±2	±8·1	±242	±15·1	±5009	±64
1000	3	40·5	13·4	443	29·8	3783	38·7	27903	224
		±23·9	±5·4	±15	±8·9	±517	±11·0	±4759	±113

Two parameters are given for closed-time components within groups. The decay rate (l) is the fitted value for the specified closed-duration component. The number of closures per second of open time (ν) is the total area of the specified component, corrected for resolution, divided by the total intracluster open time. Mean values are presented ± the standard deviation for n experiments.

component cannot be distinguished in the experimental 60 μM closed-duration histogram, as it would be masked by the more robust c_3 and c_4 components (Fig. 4). The c_2 closures are well resolved at 60 μM, and appear similar to the c_2 closures at 1 mM-ACh (decay rate of 50 s^{-1} and an occurrence rate of 11 s^{-1}). As concluded earlier in the case of the 1 mM data, the c_2 closures are not consistent with receptor activation processes.

The closed-duration histograms show little change between 130 μM- and 1 mM-ACh. The c_3 decay rate appears to reach a limiting value between 400 and 500 s^{-1}, close to the low-concentration β estimate. Over this saturating concentration range, the c_3 occurrence rate is constant, between 30 and 40 s^{-1}, consistent with the low-concentration α estimate. Some concentration-dependent changes are seen in the c_4 and c_5 components, and are discussed further below.

Fig. 5 shows the concentration dependence of β', the decay rate associated with channel opening (c_2 decay rate at 20 μM, and c_3 decay rate at 60 μM and higher). The channel opening rate increases at intermediate concentrations and shows saturation at high concentrations. The curve shown is the predicted concentration dependence of the theoretical decay rate λ_0 (see eqn. (1) and Fig. 3), predicted from the scheme (1) transition rates given in Table 2.

The transition rates in Table 2 were estimated as follows. The parameters, Q_0–Q_2 and λ_0–λ_2, were calculated for a trial set of transition rates for each ACh concentration using eqns. 3.65–3.67 given in Colquhoun & Hawkes (1981). k_{-2} was constrained to the value estimated at low ACh concentrations (1000 s^{-1}), and β was fixed to be consistent with both the low-concentration and saturating-concentration measurements (480 s^{-1}). The rates, k_1, k_2 and k_{-1}, were then varied to fit two sets of experimental observations. First, the rates were adjusted until the predicted λ_0 described the experimental concentration dependence of the β' decay rate shown in Fig. 5. Secondly, the trial rates were chosen to simulate the two activation components, c_2 and c_3, observed with 20 μM-ACh. Simulating the two 20 μM activation components amounts to fixing k_{-1} to be equal to the 20 μM c_3 decay rate. Hence, the fit in Fig. 5 was accomplished essentially by varying k_1 and k_2.

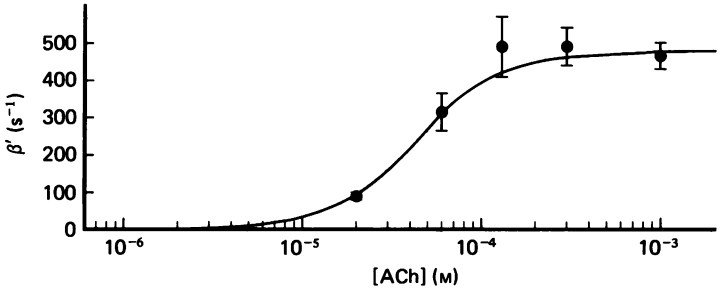

Fig. 5. Concentration dependence of the β' decay rate. Currents were recorded at the specified ACh concentrations, and the closed-duration histograms were fitted as described in the legend to Fig. 2 and Methods. The mean decay rate for the activation-related component (see text) is plotted for each concentration ± the standard deviation. The continuous curve represents the concentration dependence predicted by scheme (1) for the λ_0 component illustrated in Fig. 3. The parameters for scheme (1) are those given in the legend to Fig. 3. For the data shown, the following number of records were analysed: 20 μM, $n = 2$; 60 μM, $n = 4$; 130 μM, $n = 3$; 300 μM, $n = 2$; 1 mM, $n = 3$. $V = -70$ mV, $T = 11$ °C.

TABLE 2. Estimated rate constants

	ACh	Carbamylcholine
k_1 (M^{-1} s^{-1})	1×10^7	3×10^5
k_{-1} (s^{-1})	500	200
k_2 (M^{-1} s^{-1})	1×10^8	1×10^7
k_{-2} (s^{-1})	1000	1000
β (s^{-1})	480	150
α (s^{-1})	35	65

Estimates of rate constants for steps in scheme (1) are given for ACh and carbamylcholine. These parameters give reasonable descriptions of data obtained over a wide concentration range (see text). β and α were estimated at both high and low concentrations, k_{-2} only at low concentration, and k_1, k_{-1} and k_2 were estimated from intermediate and high concentrations. Note that k_1 and k_{-2} are not corrected for any statistical factors.

Fig. 5 shows that the effective channel opening rate, β', increases over a narrow concentration range. The agonist association rates, k_1 and k_2, are estimated to be 1×10^7 and 1×10^8 M^{-1} s^{-1} respectively (macroscopic rates). The ratio of dissociation to association rates gives estimates for ACh dissociation constants of 50 μM and 10 μM for the first and second binding steps, respectively. Inspection of Fig. 5 indicates that an even steeper curve would describe the data, consistent with dissociation constants differing as much as twentyfold. Interestingly, the different association rates account entirely for the difference in the two equilibrium dissociation constants.

As implied in the preceding analysis, the robust c_2 and c_3 components at 20 μM-ACh support the hypothesis of positive co-operativity in agonist binding. The equivalent areas of the two components suggest that a receptor in state AR is about equally likely to bind agonist and open or lose its bound agonist molecule. The relatively high occurrence rate of the c_3 closures suggests that, at 20 μM, the binding of a second ACh molecule is favoured over the dissociation of the singly occupied agonist–receptor complex (with the constants in Table 2, k_2[ACh] = 2000 s^{-1}; k_{-1} = 500 s^{-1}).

The closed-duration analysis may be summarized as follows. Two closed-duration components apparently change with agonist concentration, and are therefore suggested to reflect receptor activation processes. The decay rate of the slower component, referred to as β', increases over a narrow range of ACh concentrations and saturates at about 130 μM-ACh. This steep concentration dependence is consistent with positive co-operativity in agonist binding, with dissociation constants of 50 μM and 10 μM. The second activation component appears in the present data only at 20 μM-ACh where its area is equal to that of the β' component. Both the relatively large area and the decay rate of the second component at 20 μM-ACh are consistent with positive co-operativity in agonist binding. The co-operativity apparently arises from different agonist association rates, whereas the two dissociation rates are essentially equal. The estimated rate constants are consistent with the over-all kinetics at both high and low agonist concentrations.

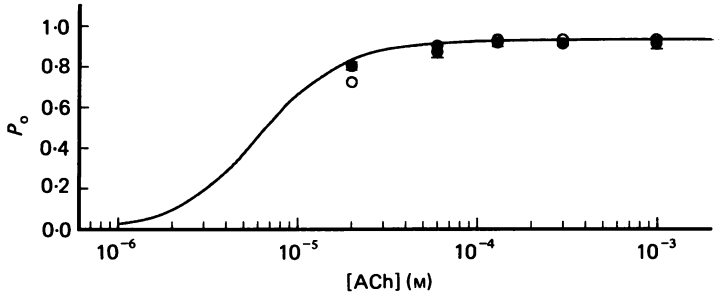

Fig. 6. Channel opening probability *versus* ACh concentration. The filled circles show the opening probability measured directly from the records with the maximum intragroup closed period set to be about four times the estimated $1/\beta'$: 40 ms for 20 μM, 20 ms for 60 μM, and 10 ms for 130 μM to 1 mM. The data plotted are mean values $\pm$ standard deviation. The open circles are the quantity, $\beta'/(\beta'+\alpha)$, where the values of β' are those plotted in Fig. 5, and α is the mean value of 35 s^{-1}. The continuous curve is the predicted P_0 for scheme (1) using the rates listed in Table 2.

Concentration dependence of the channel opening probability

The channel opening probability, P_0, also changes with the agonist concentration as shown in Fig. 6. Two estimates of the opening probability are shown: the ratio of rate constants, $\beta'/(\beta'+\alpha)$, and the measured fractional open time within groups of openings determined using a maximal intraburst interval chosen to be about four times the estimated value for β' at the given concentration (see legend to Fig. 6). The two P_0 estimates coincide closely at each agonist concentration. The continuous line through the data shows the P_0 values predicted from the set of transition rates just described, which also are consistent with the closed-time histograms. The predicted P_0 values clearly are consistent with the observed fractional open time within groups.

Possible sources for additional closed states

In the presence of 1 mM-ACh, three closed-duration components, c_2, c_4 and c_5, are observed in addition to the apparent activation component, c_3. These additional components show relatively little concentration dependence. The c_5 component resembles the agonist-independent 50 μs closures, represented as A_2R' in scheme (1).

The c_5 closures occur at a constant rate at ACh concentrations from 20 to 300 μM of 99 ± 41 per second of open time (Table 1). Although the c_5 occurrence rate is higher than the rate seen with 100 nM-ACh (50 s^{-1}, Sine & Steinbach, 1986*b*), it is probably not significantly different considering the widely variable occurrence rate seen in these high-concentration experiments (see Table 1). However, the c_5 occurrence rate increases sharply between 300 μM- and 1 mM-ACh, apparently due to fast blocking events induced ACh (Table 1). Although the decay rates differ between the agonist-independent closures and the fast blocking events (estimated to be about 20000 and 80000 s^{-1}, respectively), the two components would not be separated well enough to distinguish them as two brief exponentials using our minimum gap length of 100 μs. In addition, the duration of fast blocking events has not been measured directly at -70 mV, so our estimate could conceivably be inaccurate by several-fold. Hence, it is not surprising that the c_5 component should appear as a single exponential, even in the presence of a second fast process such as channel block. Thus, at intermediate ACh concentrations, the c_5 component arises primarily from the agonist-independent closing transition, but at saturating concentrations additional closures appear within the c_5 component, apparently due to fast block induced by ACh.

Two more closed-duration components, c_2 and c_4, are observed at high ACh concentrations, but neither component is predicted by scheme (1) under the condition of saturating agonist concentration. Both components stand out clearly at 1 mM-ACh, with time constants of about 30 ms (c_2) and 300 μs (c_4). The c_2 component appears concentration independent, showing no clear change in its time constant or frequency of occurrence at ACh concentrations above 20 μM (Table 1). The properties of the c_4 component change moderately with concentration; the decay rate and frequency of occurrence both increase about twofold between 60 μM- and 1 mM-ACh (Table 1). As noted above, the occurrence rates of the c_2 and c_4 components suggest that these closures represent dwells in closed states connected to the open-channel state. The processes resulting in the c_2 and c_4 closures are not known. The observation that the rates of occurrence do not change much over a 16-fold range of ACh concentration indicates that channel block by agonist is not likely. Further, if agonist binding to an allosteric site is involved in producing these closures, it is likely that binding to such an allosteric site is close to saturated (K_D values $\leqslant 60$ μM).

Summary of studies with a range of high ACh concentrations

To summarize the results obtained with high ACh concentrations: major closed-duration components are identified which are qualitatively well described by scheme (1). Both high- and low-concentration measurements yield similar estimates of the channel opening and closing rates, β and α. The high-concentration data also indicate positive co-operativity in agonist binding. The measured channel opening probability, P_o, is consistent with the opening probability predicted from the low-concentration measurements, and is described by scheme (1) across the range of ACh concentrations examined. In addition, a 50 μs closed-time component is observed, corresponding to the agonist-independent closed periods predicted from the low-concentration measurements, and also to fast channel block induced by saturating ACh concentrations. Two more closed-time components are observed

within groups (time constants of 300 μs and 20–30 ms), but do not appear to reflect receptor activation processes defined by scheme (1). In agreement with Sakmann *et al.* (1980), two long-duration closed dwells are seen, presumably reflecting the recovery rates of the fast and slow desensitized states.

Analysis of closed durations in the presence of high carbamylcholine concentrations

Currents induced by carbamylcholine were examined using the same strategy used to study the ACh-induced currents. Low-concentration-carbamylcholine measurements indicate β is between 150 and 190 s^{-1}, k_{-2} is about 1000 s^{-1}, and α is about 65 s^{-1} (Sine & Steinbach, 1986*b*). Carbamylcholine also has about a 20-fold lower receptor binding affinity than ACh, suggesting that concentrations up to 20 mM may be needed to achieve saturation (Weiland & Taylor, 1979; Boyd & Cohen, 1980*a*). However, carbamylcholine-induced channel block restricts the maximum carbamylcholine concentration to below about 1–2 mM (Sine & Steinbach, 1984*b*).

Fig. 7 exhibits the closed-duration histograms for a series of carbamylcholine concentrations from 180 μM to 1 mM. As is observed with ACh, the carbamylcholine closed-duration histograms are described as the sum of six exponentials: two long-duration components reflecting fast and slow desensitization recovery processes, and four short-duration components, representing potential receptor activation processes. Two of the short-duration components, c_4 and c_5, resemble the two fastest components observed with high ACh concentrations: c_5 corresponding to the agonist-independent brief closures, and c_4 to an allosteric closed state. The two remaining short-duration components, c_2 and c_3, behave qualitatively as closures predicted by scheme (1) for intermediate agonist concentrations, as though the carbamylcholine concentration never reached saturation (compare the scheme (1) predictions in Fig. 3 with Fig. 7).

Table 3 summarizes the analysis of closed-time histograms with 180 μM- to 1 mM carbamylcholine. We have tentatively identified the c_2 and c_3 components as reflecting activation. The decay rate of the c_2 component increases over a relatively narrow concentration range, but does not reach the estimate for β made at low

Fig. 7. Closed-duration histograms for a series of carbamylcholine concentrations: 180 μM, 420 μM and 1 mM at $V = -70$ mV and $T = 11$ °C. Bin sizes, left to right: 0·025, 0·4 and 3 ms. For each carbamylcholine concentration, the histogram is fitted by the sum of six exponentials. The over-all fit is shown by the upper continuous curve, while the lower dotted curves indicate the contribution of each component. The histograms show closed periods within groups. The two slowest components, c_0 and c_1, appear only as flat dotted lines in the right panel. Note that the postulated receptor activation components (c_2 and c_3) are prominent in the right and middle panels, respectively. The components are designated c_0–c_5 with decay rates, l_0–l_5, and number of events, n_0–n_5. 180 μM: $l_0 = 0{\cdot}504$ s^{-1}, $n_0 = 154$; $l_1 = 7{\cdot}32$ s^{-1}, $n_1 = 584$; $l_2 = 42{\cdot}4$ s^{-1}, $n_2 = 1707$; $l_3 = 291$ s^{-1}, $n_3 = 1195$; $l_4 = 3432$ s^{-1}, $n_4 = 1016$; $l_5 = 23153$ s^{-1}, $n_5 = 2214$. 4801 events detected, fifty-eight multiple openings, and the record length was 1690 s. 420 μM: $l_0 = 0{\cdot}339$ s^{-1}, $n_0 = 106$; $l_1 = 3{\cdot}34$ s^{-1}, $n_1 = 410$; $l_2 = 79{\cdot}6$ s^{-1}, $n_2 = 1339$; $l_3 = 335$ s^{-1}, $n_3 = 1658$; $l_4 = 2766$ s^{-1}, $n_4 = 870$; $l_5 = 22768$ s^{-1}, $n_5 = 3164$. 4618 events detected, twenty-two multiple openings, and the record length was 938 s. 1 mM: $l_0 = 0{\cdot}614$ s^{-1}, $n_0 = 304$; $l_1 = 8{\cdot}39$ s^{-1}, $n_1 = 441$; $l_2 = 99{\cdot}7$ s^{-1}, $n_2 = 1764$; $l_3 = 646$ s^{-1}, $n_3 = 1894$; $l_4 = 4198$ s^{-1}, $n_4 = 977$; $l_5 = 22387$ s^{-1}, $n_5 = 3402$. 5461 events detected, thirty-four multiple openings, and the record length was 1320 s.

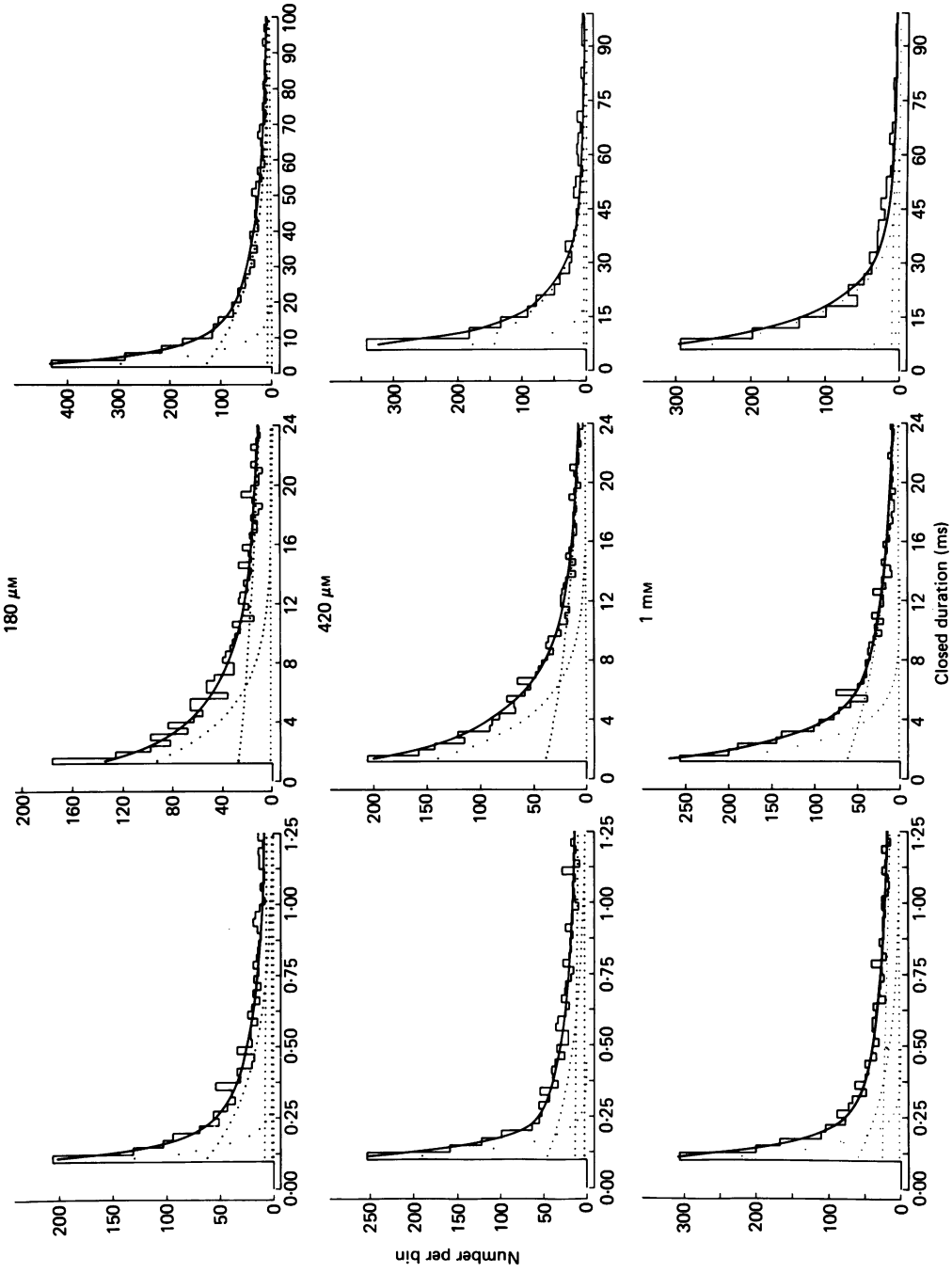

Fig. 7. For legend see opposite.

TABLE 3. Summary of carbamylcholine closed-time parameters and scheme (1) predictions

Carbamylcholine concentration (μM)	N	Rates: Predicted λ_0 (s^{-1})	Rates: Observed l_2 (s^{-1})	Rates: Predicted λ_1 (s^{-1})	Rates: Observed l_3 (s^{-1})	Ratio of areas: Predicted Q_1/Q_0	Ratio of areas: Observed A_3/A_2	Open probability, P_o: Predicted P_o	Open probability, P_o: Observed P_o	$\beta'/(\beta'+\alpha)$
180	2	25	44±3	194	375±118	0·78	1·09	0·39	0·51±0·13	0·42
420	2	69	82±5	212	285±70	0·59	1·13	0·59	0·64±0·08	0·56
1000	4	123	118±33	326	639±26	0·07	1·36±0·51	0·66	0·68±0·07	0·64

For each carbamylcholine concentration, the two predicted activation component decay rates, λ_0 and λ_1, are compared with the corresponding observed decay rates, l_2 and l_3; the predicted ratio of areas, Q_1/Q_0, is compared with the observed ratio of areas, A_3/A_2; and the predicted opening probability, P_o, is compared with the observed P_o. The predicted parameters were calculated for scheme (1) as described in the legend to Fig. 4, using the following parameters: $k_1 = 3\times10^5$ M^{-1} s^{-1}, $k_{-1} = 200$ s^{-1}, $k_2 = 1\times10^7$ M^{-1} s^{-1}, $k_{-2} = 1000$ s^{-1}, $\beta = 150$ s^{-1}. The observed decay rates and ratio of areas were obtained from the fit to closed-duration histograms such as those shown in Fig. 7. The observed P_o was measured directly from the record using a maximum of intragroup interval of 80 ms for all three concentrations. The ratio $\beta'/(\beta'+\alpha)$ was calculated from the mean l_2 decay rate at each carbamylcholine concentration and the over-all mean α of 65 s^{-1}. All observed values are presented as the mean±the standard deviation for N experiments.

carbamylcholine concentrations. This pattern resembles that of the theoretical component with decay rate λ_0 (see Fig. 3), and suggests that even 1 mM-carbamylcholine is not a saturating concentration. The c_3 component has a similar area to that of the c_2 component, and the decay rate of the c_3 component does not change greatly over the concentration range studied. The combined occurrence rate of the c_2 and c_3 components was found to be: 180 μM, $52{\cdot}7 \pm 14{\cdot}6$ s^{-1}; 420 μM, $65{\cdot}3 \pm 12{\cdot}5$ s^{-1}; 1 mM, $69{\cdot}7 \pm 13{\cdot}6$ s^{-1}. The grand mean occurrence rate is $64{\cdot}3 \pm 13{\cdot}7$ s^{-1}, very near the low-concentration α estimate of 65 s^{-1}. The channel opening probability, P_o, closely matches the scheme (1) predictions, increasing with agonist concentration, with the maximum P_o approaching the low-concentration P_o estimate. Qualitatively, then, the carbamylcholine data suggest that the experimental concentration is well below saturation, and that carbamylcholine binds less tightly to the receptor than does ACh.

As the closed-duration histograms show, the carbamylcholine-induced currents are inherently more difficult to interpret than the ACh-induced currents. First, the short-duration components are not well separated as are those with ACh (compare middle panels of Figs. 2 and 7). Hence, with carbamylcholine, the more extensive overlap of components presents difficulties in obtaining clear-cut exponential fits. Secondly, the ACh data show a concentration-independent component with a decay rate between 30 and 50 s^{-1}. With the ACh data, this concentration-independent component is well separated from the components due to receptor activation processes (except for possible overlap with the β' activation component at 20 μM-ACh). However, if a 30–50 s^{-1} component were present in the carbamylcholine closed-duration histograms, it would not be distinguished, being masked by the large β' component. The resulting β' component, then, would have both a distorted decay rate and area. Hence, due to the unfavourable disposition of closed-duration components, the carbamylcholine data must be interpreted in a semiquantitative fashion.

Despite the limitations outlined above, tentative estimates were made for the parameters in scheme (1). To estimate the scheme (1) parameters, β and k_{-2} were constrained to their low-concentration-carbamylcholine estimates as described for the ACh data. The rates k_1, k_2 and k_{-1} were then altered to yield the best match between the theoretical λ_0 and the experimental decay rate, l_2. In addition, the rates k_2 and k_{-1} were adjusted to best simulate both the decay rates and equivalent areas of the c_2 and c_3 components.

Table 3 summarizes the results of such an analysis. The transition rate estimates for scheme (1) are: $k_{-1} = 200$ s^{-1}, $k_1 = 3 \times 10^5$ M^{-1} s^{-1}, $k_{-2} = 1000$ s^{-1}, $k_2 = 1 \times 10^7$ M^{-1} s^{-1}, $\beta = 150$ s^{-1}. Using these rate constants, the concentration dependence of the observed decay rate, l_2, is described reasonably well (compare l_2 and λ_0 in Table 3). The l_3 decay rate is also well described for 180 μM- and 420 μM-carbamylcholine, but at 1 mM it is predicted to be about twofold lower than is observed (compare l_3 and λ_1 in Table 3). Finally, the ratio of observed relative areas, A_3/A_2, is close to the predictions at 180 μM and 420 μM, but at 1 mM is much larger than the predicted relative area (Q_1/Q_0). In other words, the area of the c_3 component does not decrease as predicted at 1 mM-carbamylcholine, at least for this set of rates. Several factors may account for the disparity between predicted and observed

relative areas seen with 1 mM-carbamylcholine. First, the fitting of closely spaced exponentials is inherently imprecise and may defy efforts to obtain accurate fits for the c_2 and c_3 components. A second possibility is 1 mM-carbamylcholine may be lower than a saturating concentration. Finally, the true c_3 component may have vanished at 1 mM-carbamylcholine, but carbamylcholine may induce another closed state at high concentrations. At present we cannot clearly distinguish among these possibilities. None the less, the transition rate estimates are qualitatively consistent with many features of the high-concentration carbamylcholine closed-duration histograms, and also with estimates of β, k_{-2} and α made at a low carbamylcholine concentration.

Summary of results with carbamylcholine

Although the carbamylcholine transition rate estimates are regarded as preliminary in a quantitative sense, the carbamylcholine data are consistent with some general features of receptor activation. The c_2 and c_3 closed-duration components are qualitatively consistent with scheme (1) for intermediate agonist concentrations. The idea that the experimental concentration range is intermediate is consistent with the estimated low affinity of carbamylcholine for the resting activatable receptor state (Neubig & Cohen, 1980). Finally, the high- and low-concentration carbamylcholine data are internally consistent, giving similar estimates of β, k_{-2}, α and P_o.

Kinetic homogeneity

Since several closed-duration components are present in the high-concentration-agonist closed-duration histograms, it is essential to establish that the observed components arise from a homogeneous receptor population. Therefore, the remaining sections examine the homogeneity of groups and clusters, in terms of both open and closed durations. First, the kinetic properties are examined for openings and closings within groups, excluding the rare solitary openings. Secondly, openings and closings are examined within clusters, and the kinetic properties of each cluster are compared across the entire cluster population.

Analysis of open durations

Open-duration histograms were analysed to determine the number of open states activated at high agonist concentrations. For currents induced by 1 mM-ACh, the open-duration histogram is described as the sum of two exponentials, with well-separated time constants of 13 ms and 170 μs, and fractional areas of 0·88 and 0·12, respectively (Fig. 8). In accordance with previous findings (Sine & Steinbach, 1984*a*), brief- and long-duration openings occur in about the same ratio over the range of high agonist concentrations examined (20 μM- to 1 mM-ACh; 180 μM- to 1 mM-carbamylcholine; see Table 4). Such a constant ratio supports the concept that both brief and long openings result from receptors occupied by two agonist molecules. Since two open states are clearly apparent in the data, it becomes essential to clarify the temporal relationship between brief- and long-duration open states.

Sorted open-duration histograms

Previous experiments demonstrated a temporal association between brief and long openings at high agonist concentrations (Sine & Steinbach, 1984*a*). Therefore, open-

ings were sorted according to whether they were isolated or in a group, and the corresponding open-duration histograms were constructed (see also Sine & Steinbach, 1986*a*). The fraction of grouped brief openings is also important because closed periods between brief and long openings could potentially contribute an additional component to the closed-duration histogram.

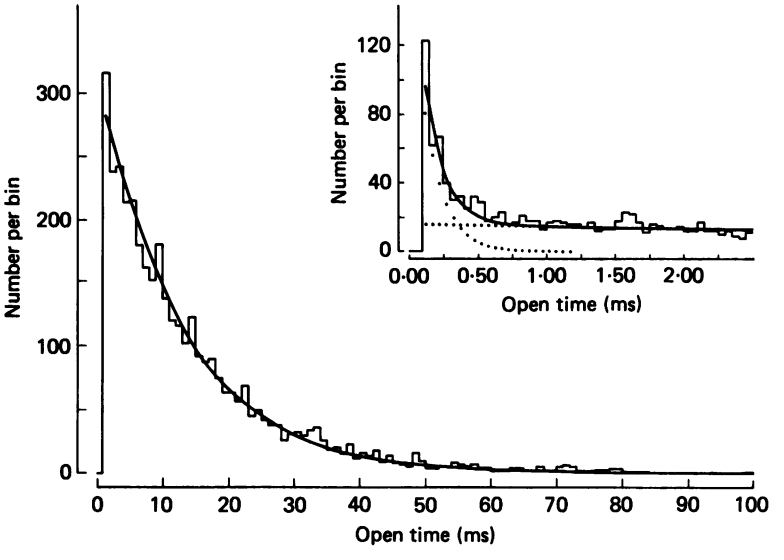

Fig. 8 Open-duration histogram of currents elicited by 1 mM-ACh at $V = -70$ mV and $T = 11$ °C. The main panel (1 ms bins) shows the distribution of long-duration openings, and the inset (0·05 ms bins) shows brief-duration openings. The histogram is fitted by the sum of two exponentials, with the continuous curve indicating the over-all fit, and the two dotted curves the contributions of each component. The fitted decay rates and number of events are: long component = 77·2 s^{-1}, 4074; brief component = 5837 s^{-1}, 509. The record analysed is the same one analysed for closed durations in Fig. 2.

To construct the sorted histograms, openings were classified as either grouped or isolated using the maximum intragroup interval used to compute the channel opening probability. The 10 ms intragroup interval was chosen to be four times $1/\beta$, the maximum closed time due to receptor activation processes. The sorting analysis reveals that about 95 % of all detected openings occur within groups of more than one opening, a percentage that remains constant over the range of agonist concentrations examined (Table 4). An example of the sorted histograms is shown in Fig. 9 for currents elicited by 1 mM-ACh. For openings within groups, the open-duration distribution is described as the sum of two exponentials with time constants of 13·8 ms and 130 μs and fractional areas of 0·91 and 0·09, respectively. Again, the fraction of grouped brief openings does not change over the range of agonist concentrations examined (Table 4). The histogram of isolated openings is described as the sum of three exponentials, with time constants of 16·0 ms, 1·3 ms, and 70 μs, and relative areas of 0·15, 0·18 and 0·67, respectively. The 1·3 ms mean-duration openings (intermediate openings) were not detected in the total open-duration histograms, presumably because of their low prevalence ($\sim$1 % of total) and intermediate mean duration. The sorted histograms show that isolated

TABLE 4. Temporal distribution of openings

Agonist concentration	Over-all fraction of long openings*	Fraction of detected openings which are in groups†	Fraction of openings in groups which are long‡
ACh			
20 μM	0·75 ± 0·11	0·94 ± 0·02	0·85 ± 0·03
60 μM	0·80 ± 0·09	0·93 ± 0·03	0·90 ± 0·05
130 μM	0·82 ± 0·06	0·95 ± 0·02	0·87 ± 0·05
300 μM	0·81 ± 0·04	0·89 ± 0·04	0·92 ± 0·02
1 mM	0·87 ± 0·01	0·95 ± 0·01	0·91 ± 0·04
Carbamylcholine			
180 μM	0·81 ± 0·04	0·96 ± 0·01	0·87 ± 0·05
420 μM	0·84 ± 0·08	0·95 ± 0·02	0·89 ± 0·06
1 mM	0·84 ± 0·06	0·96 ± 0·02	0·90 ± 0·02

* The fraction of the total openings which are long is obtained from the fit to the over-all open-duration histogram.

† Groups were defined as specified in the legends to Fig. 6 and Table 2.

‡ The fraction of the total grouped openings which are long is obtained from the fit of the open-duration histogram of grouped openings.

openings, in contrast to grouped openings, belong primarily to the short-duration-opening population.

Close coupling between brief and long openings is consistent with the following expanded receptor activation scheme:

$$2A + R \underset{k_{-1}}{\overset{k_1[A]}{\rightleftharpoons}} AR \underset{k_{-2}}{\overset{k_2[A]}{\rightleftharpoons}} A_2R \underset{\alpha}{\overset{\beta}{\rightleftharpoons}} A_2R^* \underset{b}{\overset{f}{\rightleftharpoons}} A_2R'. \qquad \text{scheme (2)}$$

$$A_2Q \underset{\alpha'}{\overset{\beta'}{\rightleftharpoons}} A_2Q^*$$

In scheme (2), receptors switch from the R to the Q states giving rise to either brief- (A_2Q^*) or long- (A_2R^*) duration openings. The present high-concentration measurements support the concept that a single receptor may switch between the R and the Q states. Therefore, the interconversion between R and Q states may introduce an additional component to the over-all closed-duration distribution. It is of interest, then, to determine the temporal distribution of closed periods between brief and long openings and to see how they influence the over-all closed-duration histogram.

Sorted closed periods within groups

To determine the temporal distribution of brief–long closures, closed intervals within groups were sorted according to their disposition between openings classified as either brief or long. Openings were classified as brief or long by establishing a discriminator time as the point of intersection of brief and long probability density functions (as determined from fitting the distribution of openings within groups). Hence, four intragroup closed-duration histograms result: closures between consecutive long events (l.l.), brief and long (b.l.), long and brief (l.b.), and consecutive brief (b.b.).

One such sorting analysis revealed the following numbers of grouped closed periods in each class for currents activated by 1 mM-ACh: l.l. = 3456, l.b. = 202, b.l. = 202, b.b. = 20. For l.l. intragroup closures, the histogram is described as the sum of three exponentials plus a constant (Table 5). These three components closely resemble the c_5, c_4 and c_3 components seen in the over-all 1 mM closed-duration histogram (see Fig. 2). For closures separating heterogeneous openings (l.b. plus b.l.), the histogram is also described as the sum of three exponentials plus a constant (Table 5). The l.b. plus b.l. distribution closely resembles the three components seen in both the l.l. distribution and in the over-all histogram. The similarity between the l.l. and the l.b. plus b.l. sorted histograms shows that brief openings in groups do not directly contribute a distinct component to the over-all closed-duration histogram. Instead, closed periods between brief and long openings are indistinguishable from those between long openings.

TABLE 5. Parameters for the sorted closed-time distributions for 1 mM-ACh

Closure classification	c_3' (s^{-1})	n_3'	c_4' (s^{-1})	n_4'	c_5' (s^{-1})	n_5'
l.l.	359±26	0·14±0·08	3407±200	0·14±0·04	24373±4725	0·72±0·12
l.b.+b.l.	321±45	0·22±0·09	2214±585	0·10±0·05	25508±3623	0·68±0·12

The classification, l.l., refers to closures between consecutive long openings, whereas l.b.+b.l. refers to closures between heterogeneous openings (see text). The parameters c_3'–c_5' are the decay rates fitted to the closed-duration histogram, and are analogous to the c_3–c_5 components in Fig. 2. The fractions n_3'–n_5' represent the fraction of the total events for each component. The entries are the mean ± the standard deviation for three experiments.

The interpretation of sorted closed periods is not clear-cut because some apparent brief openings originate from the long-duration-opening population through event misclassification. For the data illustrated in Fig. 9, seventy-two long openings fall within the brief window (0·1–0·35 ms) or 35% of the classified brief openings. Therefore, about 35% of the l.b. plus b.l. closures are really l.l. closures, accounting for some of the similarity between the two sorted distributions. However, only twenty-seven brief openings are mistaken as long, or 0·7% of the classified long openings. Thus, the l.l. closed dwell times, which are not significantly influenced by event misclassification, exhibit the same three exponentials characteristic of the original closed-duration histogram. Closed periods between brief and long openings, then, do not directly influence these three major closed-duration components.

Although the distributions appear equivalent for closed durations bounding either brief or long openings in groups, the existence of a closely coupled brief open state could indirectly influence the distribution of closed durations between consecutive long openings in groups. Potentially, closures between long openings may originate through transitions between the A_nR and the A_nQ states without ever reaching the brief open state (A_2Q^*). Such a transition sequence would lead to a compound closed period separating two long openings (i.e. $A_2R^* \rightarrow A_2R \rightarrow A_2Q \rightarrow A_2R \rightarrow A_2R^*$). Therefore, although brief openings are quite rare, they could indirectly lead to some of the closures seen in the over-all closed-duration histogram. It is not known whether such compound closed periods occur in the present data.

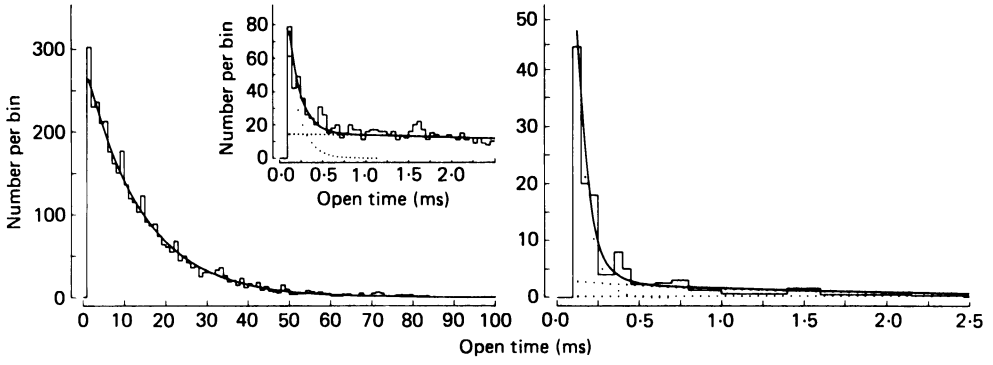

Fig. 9. Sorted open-duration histograms for currents elicited by 1 mM-ACh. Left panel: openings within groups sorted using a maximum intragroup interval of 10 ms (main panel, bin size: 1 ms; inset 0·05 ms). Right panel: isolated openings (bin size: 0·05 ms). The open-duration distribution in groups is the sum of two exponentials with the following decay rates and total events: long, 72·6 s^{-1}, 4035; brief, 7492 s^{-1}, 414. The isolated opening distribution is fitted by the sum of three exponentials: long, 62·4 s^{-1}, 65; intermediate, 764 s^{-1}, 81; brief, 14521 s^{-1}, 363. The sorting analysis classified 4282 grouped openings and 204 as isolated openings. The record analysed is the same one analysed in Figs. 2 and 8.

Distribution of the number of openings per group

Potentially, distinct types of groups might arise with different numbers of openings per group. Thus the distribution of the number of openings per group was examined as a test for group homogeneity (see also Sine & Steinbach, 1986*b*). As described above, a group is defined as any sequence of openings separated by closures shorter than 10 ms for 1 mM-ACh. Fig.10 shows that the number of openings per group is described by a single geometric distribution with many openings per group, plus a surplus of solitary openings. The extrapolated number of isolated long-duration openings is close to the fraction of long openings observed in the corresponding open-duration histogram (see Fig. 10). This result is consistent with the sorted opening analysis which shows that solitary openings belong primarily to the short-duration-opening population. Each experiment revealed a single geometric distribution for groups with more than one opening. Groups of openings, therefore, appear kinetically homogeneous in the sense that the probability of reopening quickly (within 10 ms of a closing) is constant across all groups.

Homogeneity of clusters of openings

Clusters of openings were analysed to determine whether the activity in a patch appeared homogeneous at this level. Further, if a cluster represents the repeated activity of a single ACh receptor, some comparisons may be made between the properties of individual receptors in a patch. The analysis is limited by the complexity of the closed-time histograms: although a cluster may contain up to 300 openings this still does not allow an accurate analysis of closed-time distributions within a cluster. In all, twelve runs were analysed (ACh concentrations of 130, 300 and 1000 μM and carbamylcholine concentration of 1000 μM).

A cluster was defined as a series of openings separated by closed periods of less than

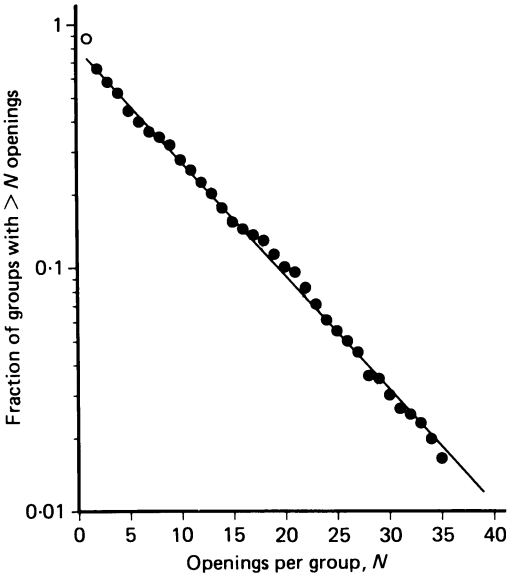

Fig. 10. The fraction of total groups with N or more detected openings is plotted semilogarithmically against N. The openings were elicited by 1 mM-ACh (same record illustrated in Figs. 2, 8 and 9), and were analysed using a maximum intragroup closed period of 10 ms. The data are fitted using a linear least-squares routine for groups containing more than one opening. The open circle at one or more openings represents the fraction of total openings which are long duration, obtained by fitting the total distribution of open times (Fig. 8). Note that the data are well described by a single geometric distribution for groups with multiple openings, and that most of the excess single-event groups are due to isolated short-duration openings.

2 s (changing this time from 1 to 4 s did not alter the results of the analysis described, although different numbers of clusters were identified). Within a cluster, groups were defined as a series of openings separated by closed periods of 10 ms or less, and openings were defined by the minimum closed period (100 μs). When plots similar to Fig. 10 were made for the distribution of clusters with N or more openings (or N or more groups of openings), the data were well described by a single geometric distribution (data not shown). These observations suggest that clusters are relatively homogeneous in terms of the probability that a receptor will reopen a short time after a closing, or will reopen from a relatively long-lived closed state.

A somewhat more refined analysis is illustrated in Fig. 11 for one run with 1 mM-ACh. Thirty-six clusters were identified in this data set. The four panels of Fig. 11 show the mean open time and some properties of brief closures for each of these clusters. The mean open times appear to differ between various clusters. This possibility was tested using the likelihood ratio test (Lawless, 1982; Patlak, Ortiz & Horn, 1986). The results of this test indicated that it is extremely unlikely that all of the clusters in this record have the same mean open time ($P < 0{\cdot}005$ for this experiment). It is possible that the differences arise because some clusters have a larger proportion of brief openings than others. The data shown in Fig. 12 demonstrate that this cannot explain the results of the likelihood ratio test. A cluster with a short

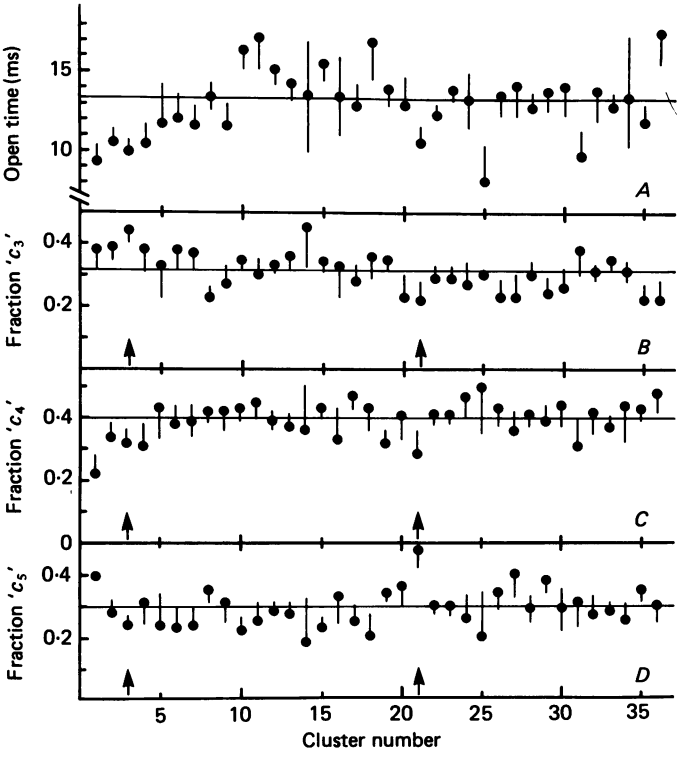

Fig. 11. Homogeneity of clusters elicited by 1 mM-ACh. Clusters were identified using a maximum intracluster closed period of 2 s, and had to contain at least ten openings, yielding a total of thirty-six clusters (same record shown in Figs. 2, 8, 9 and 10). *A*, mean open time per cluster. The bars give an estimate of the error of the estimate (S.D./$\sqrt{n}$) for each cluster. The horizontal line gives the grand mean open time (13·25 ms, $n = 4285$). Brief closures within clusters were classified as 'c_3 gaps' (*B*, 0·7 ms $\leqslant d <$ 10 ms), 'c_4 gaps' (*C*, 0·15 ms $\leqslant d <$ 0·7 ms) or 'c_5 gaps' (*D*, 0·1 ms $\leqslant d <$ 0·15 ms). Data for each class of brief closures are shown as the fraction of the total closures lasting less than 10 ms in each cluster. The horizontal line shows the over-all proportion for all of the brief closures counted in the record. The vertical bars give an estimate of the error in the fraction, $E_{i,j} = \sqrt{(f_i(1-f_i)/N_j)}$ where $E_{i,j}$ is the variability in the estimate for the ith class of the jth cluster, f_i is the over-all fraction of the total brief closures in the ith class, and N_j is the total number of closures less than 10 ms long in the jth cluster. The arrows in *B*, *C* and *D* mark clusters for which the brief closures had significantly different proportions than the over-all population.

mean open time and one with a long mean open time show distributions of open times dominated by single-exponential components with quite different means. The lower panel of Fig. 12 shows a frequency distribution of the mean open times for the thirty-six clusters in this experiment. The histogram is reasonably described by a Gaussian curve with mean 13·1 ms and standard deviation 2·2 ms. Over-all, the data from this experiment strongly suggest that individual ACh receptors do not have identical mean open times. The results of the likelihood ratio test were similar in most experiments: eight of twelve experiments had $P < 0{\cdot}005$, three had $P < 0{\cdot}05$ and only one had a $P > 0{\cdot}1$ that differences in mean open times between clusters arose by chance.

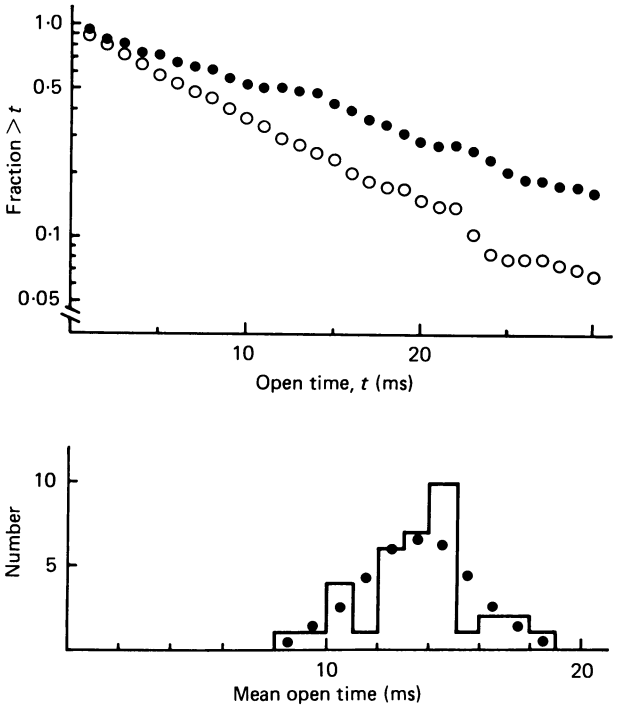

Fig. 12. Open times in clusters. The upper panel shows a semilogarithmic plot of the fraction of openings with durations longer than the abscissal value for two clusters of the experiment illustrated in Fig. 11. Cluster 3 (open circles, $n = 222$, mean open time 9·97 ms) has a relatively short mean open time whereas cluster 11 (filled circles, $n = 228$, mean open time 17·2 ms) has a long mean open time. Note that both sets of data are quite close to linear on this semilogarithmic plot, with different slopes. (For cluster 3, the inverse of the slope is 10·3 ms; for cluster 11, 16·4 ms). The lower panel shows a histogram of the mean open times for the thirty-six clusters in this experiment, with a calculated Gaussian superimposed (13·17 ± 2·22 ms). The data are reasonably described by the Gaussian curve.

However, clusters with differing mean open times did not show major or consistent differences in closed periods within groups.

The closed periods within clusters were analysed by defining four duration intervals, d: 0·1 ms $\leqslant d <$ 0·15 ms ('c_5 gaps'), 0·15 ms $\leqslant d <$ 0·7 ms ('c_4 gaps'), 0·7 ms $\leqslant d <$ 10 ms ('c_3 gaps') and 10 ms $\leqslant d <$ 2 s ('c_2 gaps' and 'c_1 gaps'). The numbers of closed periods falling in each interval were determined for each cluster and for the record as a whole. Since the focus of this study is on relatively brief closures the data were analysed in terms of the fraction of closures lasting less than 10 ms which fell in the 'c_5 gap', 'c_4 gap' and 'c_3 gap' intervals. The null hypothesis is that the probability of a brief closure falling in a given interval is constant across the record. This hypothesis was tested by calculating the over-all fraction of brief closures in the entire record which fell into the ith window (e.g. f_5 = (number of closures with 0·10 ms $\leqslant d <$ 0·15 ms)/(number of closures lasting less than 10 ms)). For each cluster, the expected number of closures in each class was predicted from the fraction found in the record as a whole and the total number of closures in the

cluster which lasted less than 10 ms ($N_{i,j} = f_i N_j$; ith class and jth cluster). Predicted and observed numbers were compared by calculating χ^2 and determining its probability of occurrence for two degrees of freedom. The majority of clusters had χ^2 values within the expected range (i.e. the distribution of observed χ^2 values conformed well to the distribution of χ^2 with two degrees of freedom). In this experiment, however, two clusters (indicated in the Figure by arrows) had $\chi^2 > 13$ ($P < 0{\cdot}005$). These clusters had relatively short mean open times, but otherwise had no features in common (compare lower panels of Fig. 11). In three other experiments there were single clusters with χ^2 values giving $P < 0{\cdot}01$. The conclusion from these observations is that the majority of clusters in an experiment appeared to be homogeneous in terms of the relative proportions of 'c_3 gaps', 'c_4 gaps' and 'c_5 gaps' within the cluster. Those clusters which deviated significantly had no consistent pattern of properties.

Inspection of Fig. 11 indicates that there is no strong correlation between the mean open time in a cluster and the proportions of classes of brief closures. No correlation was apparent in any of the runs analysed.

In over-all summary, there is evidence to support the idea that the mean open times differ between clusters, and therefore that individual ACh receptors differ in their mean open times at high agonist concentrations (ACh above 100 μM, carbamylcholine at 1 mM). The interpretation of this conclusion is not obvious, however, since there is no strong correlation between the mean open time and the prevalence of a particular class of brief closing. Over-all, the clusters are largely homogeneous in terms of the prevalence of different classes of brief closures. The observation that a few clusters appear to differ significantly from the rest in an experiment cannot be interpreted, largely because such clusters are few and do not have particular features in common.

DISCUSSION

The present study describes the activation of ACh receptors on clonal BC3H–1 cells by high concentrations of two strong agonists, ACh and carbamylcholine. Combined with the results from low-agonist-concentration measurements (Sine & Steinbach, 1986*b*), these findings lead to the following proposed picture for receptor activation. The receptor consists of two binding sites linked to one channel, and both sites must bind the agonist for the channel to open. The first site binds the agonist at a relatively slow rate (and with a low affinity), but once occupied, the second agonist binds at a twentyfold faster rate. With both sites occupied the opening probability is high, and the channel opens within a few milliseconds. The open channel persists for tens of milliseconds. The rate constants for channel opening and for agonist dissociation are of comparable magnitude, so at low concentration, a doubly occupied receptor opens, on average, more than once. Over-all, the ACh receptor on BC3H–1 cells behaves in a fashion appropriate for receptors at the neuromuscular junction. The agonist dissociation rate is fairly large, so that bound ACh will not persist for long periods of time after a transient increase of the ACh concentration. The fast dissociation rate results in a fairly large dissociation constant. The apparent positive co-operativity in agonist binding results in a steep increase in the fraction

of receptors which are doubly liganded over a relatively narrow range of ACh concentrations. Doubly liganded receptors have a high probability of having an open channel ($\beta/(\beta+\alpha) = 0{\cdot}93$). However, because of the relatively large value for k_{-2} and low value for β, at low agonist concentration the probability that the channel of a closed and doubly liganded receptor will open ($\beta/(\beta+k_{-2})$) is only 0·32.

Although the ACh receptors on BC3H–1 cells behave qualitatively as expected for ACh receptors at adult mammalian neuromuscular junctions, there are significant quantitative differences. Basically, the BC3H–1 receptors appear to be slower than junctional ACh receptors. The burst duration and estimated $1/\alpha$ are both longer than the time constant for miniature end-plate current (m.e.p.c.) decays, indicating that α must be larger for adult receptors (e.g. Linder, Pennefather & Quastel, 1984). Similarly, our estimates of β and k_{-2} would produce an m.e.p.c. which rose more slowly than is observed (Linder *et al.* 1984; for further discussion, see Sine & Steinbach, 1986*b*). Colquhoun & Sakmann (1985) have studied the AChR at frog neuromuscular junctions; their estimates for β, α and k_{-2} are all roughly an order of magnitude larger than ours. Leibowitz & Dionne (1984), on the other hand, made estimates of β and k_{-2} comparable to ours in studies of receptors at snake junctions. Over-all, the kinetic behaviour of the AChR on BC3H–1 cells is more consistent with results obtained studying neonatal mammalian muscle (Sakmann & Brenner, 1978; Steele & Steinbach, 1986).

The preceding interpretation rests on the analysis of closed-duration histograms at high agonist concentrations and on the identification of closed dwell times corresponding to processes described by a simple receptor activation scheme (scheme (1)). However, both the open- and closed-duration histograms show more components than predicted by scheme (1). At present, the functional significance is unknown for these additional states. They are considered further below.

Although the closed-duration histograms exhibit more than the predicted number of components for a simple receptor activation scheme, the histograms do appear to reflect the activity of a homogeneous receptor population. In the present experiments, receptor activation is studied in cells a short time after inducing differentiation. In these relatively young BC3H–1 cells, only a single conductance class of channels is observed and subconductance states are rarely detected. The kinetics of groups appear homogeneous in the sense that the number of openings per group is described by a single geometric distribution. Clusters also appear to be generally homogeneous, although mean open times do differ between clusters. The proportions of brief closures appear to be generally constant across clusters. Thus, it is reasonable to interpret the closed-time histograms under the assumption that the receptor population is homogeneous.

Despite their complexity, the closed-duration histograms at high agonist concentrations exhibit two major closed-time components consistent with a simple receptor activation mechanism as represented by scheme (1). First, there is a prominent concentration-dependent component with a decay rate, β', that increases at intermediate ACh concentrations and shows saturation at high concentrations. The saturating value, then, is the high-concentration estimate of β, the channel-opening rate constant, which agrees well with the β estimate obtained from independent low-concentration ACh experiments. Although the carbamylcholine

data are more difficult to interpret, an analogous β' component is also observed with a decay rate that increases with concentration and is consistent with the corresponding low-concentration β estimate. A second apparent activation component is distinguished clearly at intermediate agonist concentrations with an area comparable to that of the β' component. At saturating ACh concentrations, the second activation component apparently vanishes, as predicted by scheme (1). The quantitative features of the second activation component combine with the concentration dependence of the β' component to give estimates of the rates, k_1, k_2 and k_{-1}. Thus, for ACh, transition rates are presented for scheme (1) which accurately simulate both the concentration dependence of the β' component and the relative areas and decay rates of the two apparent activation components seen with 20 μM-ACh.

The rate constants, k_1, k_2 and k_{-1}, were estimated under the assumption that the observed closed-duration components correspond to the components predicted by scheme (1). We fixed the value of β to be consistent with the similar estimates from both the low- and high-agonist-concentration measurements. Similarly, k_{-2} was fixed to the value estimated from the low-concentration measurements. For ACh, the association rates, k_1 and k_2, are estimated to be up to twentyfold different, and appear to be the major source of positive co-operativity in agonist binding. The k_2 estimate of 1×10^8 M^{-1} s^{-1} approaches diffusion limits, and is similar to the association rate reported for ACh binding to the high-affinity desensitized state of the receptor (Boyd & Cohen, 1980*b*) and the association rates for NBD-5-acylcholines (Prinz & Maelicke, 1983). Although much less firm, the two association rates for carbamylcholine also appear to be different, but are estimated to be about tenfold lower than those for ACh. For ACh, the first agonist dissociation rate, k_{-1}, is estimated to be about 500 s^{-1}, essentially identical to $k_{-2}/2$, the microscopic dissociation rate for the fully occupied receptor. Two experimental observations support the k_{-1} estimate. First, two activation components occur with about the same probability at the intermediate ACh concentration of 20 μM. With the chosen values of k_{-1} and k_2, an equivalent occurrence probability is predicted for the two activation components. Secondly, k_{-1} may be estimated directly from the decay rate of the c_3 component at 20 μM-ACh, giving a value of 560 s^{-1}. Thus, the two agonist dissociation rates are similar and show no dependence on the degree of agonist occupancy. In contrast, the two association rates appear to be different, being the primary source of positive binding co-operativity.

Although the results support the general idea of positive co-operativity in agonist binding, the estimated degree of co-operativity is less certain. The major source of uncertainty lies in fitting a multi-exponential closed-time histogram, a problem which is minimized when the components are well separated as they are with ACh. A related problem arises when components with small areas are not recognized as such but overlap with larger, apparently clearly resolved components. Closely spaced components, then, may cause misleading decay rate estimates. For example, with ACh a small but clear-cut concentration-independent component is seen with a decay rate of 30–50 s^{-1}, which is resolved at concentrations between 60 μM and 1 mM, but not at 20 μM. Since it is concentration independent, it does not appear to be involved in receptor activation processes. However, if it were present at 20 μM, it would overlap

with the β' activation component (apparent decay rate of 90 s^{-1}). The overlap, then, would lead to an underestimate of the β' decay rate, giving an apparently greater degree of positive co-operativity. However, we have presented a lower limit of fivefold for the ratio of dissociation constants, noting that up to a twentyfold difference in K_D values fits the data equally well. Moreover, the robust second activation component seen with 20 μM-ACh provides independent evidence for binding co-operativity, as it is predicted to be much smaller for non-co-operative binding. Potential fitting errors are more serious with the carbamylcholine data because the brief components are more closely spaced and a small 30–50 s^{-1} component would not be resolved at any of the concentrations used. None the less, an unresolved 30–50 s^{-1} component would probably lead to an underestimate of the true degree of positive co-operativity because it would increase the apparent β' decay rate at low carbamylcholine concentrations and decrease it at high concentrations. Again, the presence of a prominent second activation component provides additional support for binding co-operativity. However, due to the interference from agonist-induced channel block, we have not been able to raise the carbamylcholine concentration high enough to extinguish this potential second activation component as we have done with ACh. The over-all data support the idea of positive binding co-operativity and lower-limit estimates are presented for the degree of co-operativity.

Once the probable activation components were identified it was then possible to estimate the channel closing rate, α, and the opening probability, P_0. For both ACh and carbamylcholine, the high-concentration (1 mM) estimates of α and P_0 agree well with the corresponding low-concentration estimates. In addition, scheme (1) describes the concentration dependence of P_0 using the transition-rate estimates obtained from the analysis of the closed-duration histograms. Thus, the close correspondence between high- and low-concentration estimates of α and P_0 supports the identification of the activation components in the closed-duration histograms.

It is well established that the two receptor-ligand recognition sites are not equivalent (Damle & Karlin, 1978; Sine & Taylor, 1980), even though the two α subunits of the AChR have the same amino acid sequence (Noda, Takahashi, Tanabe, Toyosato, Furutani, Hirose, Asai, Inayama, Miyata & Numa, 1982). For the classical antagonist, (+)-dimethyltubocurarine, the sites are distinguishable before the antagonist binds, and this affinity difference is preserved following antagonist attachment (Sine & Taylor, 1980, 1981). The two sites also appear initially distinguishable before agonist binding (Sine & Taylor, 1980), but the present data indicate that the affinity also changes following agonist occupancy. The initial non-equivalence of sites for both agonists and antagonists would generate apparent negative co-operativity in binding, but may be reconciled with the present data supporting positive binding co-operativity for agonists. For instance, suppose the sites were initially distinguishable for agonists as the binding data suggest. The agonist would first bind to the original high-affinity site, and then induce the neighbouring empty site to switch from low to high affinity. Therefore, the original low-affinity site ultimately binds the agonist with a very high affinity. Thus, the combination of initially distinguishable sites and positive binding co-operativity implies an ordered sequence of binding events leading to receptor channel opening. It is not known

whether agonist dissociation is ordered, although the present interpretation of the data suggests that it is random.

The parameter estimates for scheme (1) can be used to predict the macroscopic concentration dependencies for agonist binding and for agonist-induced channel activation. The transition-rate estimates for ACh predict that 50 % of the sites will be occupied at 6·7 μM and 50 % of the channels will be open at 13·7 μM ($T = 11$ °C, $V = -70$ mV). Although binding and activation measurements have not been done with ACh on BC3H–1 cells, the predicted concentration for 50 % activation is close to values measured in other systems: 80 μM for ^{86}Rb efflux from *Electrophorus electricus* vesicles at $T = 1$ °C and $V \simeq 0$ mV (Cash *et al.* 1981); 29 μM for voltage-clamped frog neuromuscular junctions at $T = 20$ °C and $V = -80$ mV (Dreyer, Peper & Sterz, 1978). The less certain parameters for carbamylcholine predict 50 % occupancy at 142 μM and 50 % activation at 316 μM. For BC3H–1 cells, carbamylcholine binding measurements show 50 % occupancy at 120 μM following short-term carbamylcholine exposure, and tracer-ion flux measurements show 50 % activation at 75 μM at $T = 11$ °C and $V \simeq 0$ mV (S. M. Sine, unpublished measurements; see also Sine & Taylor, 1980 for 3·5 °C measurements). These macroscopic binding and flux measurements are expected to underestimate the true half-maximal concentrations because relatively long times (15 s) were used to make the binding and flux measurements, allowing desensitization to develop during the measurement process. For carbamylcholine, the predicted concentration for eliciting 50 % activation is also close to the values obtained in other systems which achieve time resolution into the millisecond range: 600 μM for ^{22}Na efflux from *Torpedo* post-synaptic vesicles at $T = 4$ °C and $V \sim 0$ mV (Neubig & Cohen, 1980); 268 μM for voltage-clamped frog neuromuscular junctions at $T = 15$ °C and $V = -70$ mV (Dionne, Steinbach & Stevens, 1978).

In addition to the apparent activation components, four more closed-duration components are observed within clusters, with time constants of 50 μs, 300 μs, 20–30 ms, and 100–500 ms. At all high concentrations examined, the 50 μs closures have about the same mean duration as the agonist-independent closures observed at low agonist concentrations. Also, at intermediate agonist concentrations (20–130 μM-ACh; 180–1 mM-carbamylcholine), the 50 μs closures occur at a rate of about 90 per second of open time which is similar to the rate observed at low concentrations ($\sim$ 50–60 s^{-1}). At saturating ACh concentrations, the 50 μs closures occur at a higher rate, apparently because fast block by ACh causes the appearance of additional very brief closures. Such a qualitative concentration dependence for fast block is consistent with other studies of channel block (Sine & Steinbach, 1984*b*). If the low-concentration 50 μs closures were to reflect receptor activation processes, scheme (1) predicts changes in their properties at high agonist concentrations. However, the interference of agonist-induced block at very high agonist concentrations makes this a difficult prediction to test fully. Over-all, the present high-concentration data are compatible with the low-concentration data which suggests the 50 μs closures represent an intrinsic closed-state characteristic of open channels, and this closed state is independent of both the nature of the agonist and its concentration (see also Sine & Steinbach, 1986*a*).

Three more closed states are observed within clusters of openings. The first

component, c_1, is not observed at limiting low agonist concentrations. The c_1 time constant, 100–500 ms, is similar to that of the 'interburst intervals' described by Sakmann *et al.* (1980) which reflect the recovery rate of a single receptor from the rapidly recovering desensitized state. The second component, c_2, has a time constant between 20 and 30 ms, and an area about one-fourth the area of the β' component. Neither its time constant nor its relative area change between 60 μM and 1 mM, suggesting that the c_2 closures may reflect an additional desensitized state (e.g. the 'pre-desensitized state' suggested by Magleby & Pallotta, 1981). The third component, c_4, also is not apparent at low agonist concentrations. The c_4 component appears clearly at high agonist concentrations with an area comparable to that of the c_3, or the β' component. The occurrence frequency of c_4 closures increases moderately with increasing agonist concentration, but not enough to be due to slow channel block by the agonist. Instead the c_4 closures more likely result from a closed state induced allosterically at raised agonist concentrations. Since the c_1, c_2 and c_4 components are observed at what must be considered a saturating ACh concentration, it seems likely that they represent doubly occupied closed states in addition to those predicted by scheme (1). By analogy to the agonist-independent 50 μs closures, these additional closed states may represent a family of endogeneous inactive states reached through branch points from scheme (1).

We have previously described experiments showing that there are two, and under some conditions, three components in the open-duration histograms (Sine & Steinbach, 1984*a*, 1986*a*, *b*). Both the earlier and the present data show that doubly occupied receptors give rise to both brief and long openings, and that a single receptor may switch to either open state. The temporal association between brief and long openings leads to an expanded receptor activation scheme (scheme (2)) in which the receptor may adopt a second activatable state, A_2Q, and produce brief openings, A_2Q^*. There also appears to be another closed state which underlies the long closed periods bounding the isolated brief openings. Such isolated brief openings at high concentrations may represent the rare activity of desensitized receptors. Colquhoun & Sakmann (1985) have also observed an excess of brief openings for receptors at frog neuromuscular junctions. They have found that at very low agonist concentrations, the fraction of brief openings decreases with increasing agonist concentration as would be predicted if singly occupied receptor channels were to open for brief durations. However, at intermediate concentrations an excess of brief openings persists at a relatively constant proportion, as we have found. Multiple classes of openings would be expected to affect the distribution of closed times, as mentioned earlier in Results. At present, it seems reasonable to assume that the distribution of closed times within groups is not greatly distorted by brief openings, since almost all openings within groups are of long duration.

In summary, the activation of the ACh receptor on BC3H–1 cells shows many features of a simple linear activation scheme. This interpretation is based on the over-all agreement obtained in studies of several agonists at low concentration (Sine & Steinbach, 1986*a*, *b*) and the present results concerning activation by high concentrations of two agonists. However, it is equally clear that a single receptor molecule may adopt additional open and closed states. Scheme (1), therefore, forms the basic core description of the receptor activation process, while additional

activatable states are reached through branch points in this simple scheme. The functional significance is unknown for what appear to be extra receptor states, although they seem to reflect the activity of a doubly occupied receptor.

S.M.S. was supported by a N.I.H. post-doctoral fellowship. The research was supported by N.I.H. grants NS-13719 and NS-22356. We thank Drs D. Colquhoun and B. Sakmann for discussions and for copies of manuscripts prior to publication.

REFERENCES

BOYD, N. D. & COHEN, J. B. (1980*a*). Kinetics of binding of ^{3}H-acetylcholine and ^{3}H-carbamylcholine to *Torpedo* postsynaptic membranes: slow conformational transitions of the cholinergic receptor. *Biochemistry* **19**, 5344–5353.

BOYD, N. D. & COHEN, J. B. (1980*b*). Kinetics of binding of ^{3}H-acetylcholine to *Torpedo* postsynaptic membranes: association and dissociation rate constants by rapid mixing and ultra filtration. *Biochemistry* **19**, 5353–5358.

CASH, D. J., AOSHIMA, H. & HESS, G. P. (1981). Acetylcholine-induced cation translocation across cell membranes and inactivation of the acetylcholine receptor: chemical kinetic measurements on the millisecond time region. *Proceedings of the National Academy of Sciences of the U.S.A.* **78**, 3318–3322.

COLQUHOUN, D. & HAWKES, A. G. (1981). On the stochastic properties of single ion channels. *Proceedings of the Royal Society* B **211**, 205–235.

COLQUHOUN, D. & SAKMANN, B. (1985). Fast events in single-channel currents activated by acetylcholine and its analogues at the frog muscle end-plate. *Journal of Physiology* **369**, 501–557.

DAMLE, V. & KARLIN, A. (1978). Affinity labeling of one of two α-neurotoxin binding sites in the acetylcholine receptor from *Torpedo californica*. *Biochemistry* **17**, 2039–2045.

DIONNE, V. E., STEINBACH, J. H. & STEVENS, C. F. (1978). An analysis of the dose–response relationship at voltage-clamped frog neuromuscular junctions. *Journal of Physiology* **281**, 421–444.

DREYER, F., PEPER, K. & STERZ, R. (1978). Determination of dose–response curves by quantitative ionophoresis at the frog neuromuscular junction. *Journal of Physiology* **281**, 395–419.

LAWLESS, J. F. (1982). *Statistical Models and Methods for Lifetime Data*. New York: J. Wiley and Sons.

LEIBOWITZ, M. D. & DIONNE, V. E. (1984). Single-channel acetylcholine receptor kinetics. *Biophysical Journal* **45**, 153–164.

LINDER, T. M., PENNEFATHER, P. & QUASTEL, D. M. J. (1984). The time course of miniature endplate currents and its modification by receptor blockade and ethanol. *Journal of General Physiology* **83**, 435–468.

MAGLEBY, K. S. & PALLOTTA, B. S. (1981). A study of desensitization of acetylcholine receptors using nerve-released transmitter in the frog. *Journal of Physiology* **316**, 225–250.

NEUBIG, R. & COHEN, J. (1980). Permeability control by cholinergic receptors in *Torpedo* postsynaptic membranes: agonist dose–response relations measured at second and millisecond times. *Biochemistry* **19**, 2770–2779.

NODA, M., TAKAHASHI, H., TANABE, T., TOYOSATO, M., FURUTANI, Y., HIROSE, T., ASAI, M., INAYAMA, S., MIYATA, T. & NUMA, S. (1982). Primary structure of the alpha-subunit precursor of the *Torpedo californica* acetylcholine receptor deduced from the cDNA sequence. *Nature* **299**, 793–797.

PATLAK, J. B., ORTIZ, M. & HORN, R. (1986). Opentime heterogeneity during bursting of sodium channels in frog skeletal muscle. *Biophysical Journal* **49**, 773–777.

PRINZ, H. & MAELICKE, A. (1983). Interaction of cholinergic ligands with the purified acetylcholine receptor protein. II. Kinetic studies. *Journal of Biological Chemistry* **258**, 10273–10282.

SAKMANN, B. & BRENNER, H. (1978). Change in synaptic channel gating during neuromuscular development. *Nature* **276**, 401–402.

SAKMANN, B., PATLAK, J. & NEHER, E. (1980). Single acetylcholine activated channels show burst-kinetics in the presence of desensitizing concentrations of agonists. *Nature* **286**, 71–73.

SINE, S. M. & STEINBACH, J. H. (1984*a*). Activation of a nicotinic acetylcholine receptor. *Biophysical Journal* **45**, 175–185.

SINE, S. M. & STEINBACH, J. H. (1984*b*). Agonists block currents through acetylcholine receptor channels. *Biophysical Journal* **46**, 277–284.

SINE, S. M. & STEINBACH, J. H. (1986*a*). Acetylcholine receptor activation by a site-selective ligand: nature of brief open and closed states in BC3H–1 cells. *Journal of Physiology* **370**, 357–379.

SINE, S. M. & STEINBACH, J. H. (1986*b*). Activation of acetylcholine receptors on clonal mammalian BC3H–1 cells by low concentrations of agonist. *Journal of Physiology* **373**, 129–162.

SINE, S. M. & TAYLOR, P. (1980). The relationship between agonist occupation and the permeability response of the cholinergic receptor revealed by bound cobra α-toxin. *Journal of Biological Chemistry* **255**, 10144–10156.

SINE, S. M. & TAYLOR, P. (1981). Relationship between reversible antagonist occupancy and the functional capacity of the acetylcholine receptor. *Journal of Biological Chemistry* **256**, 6692–6699.

STEELE, J. A. & STEINBACH, J. H. (1986). Single-channel studies reveal three classes of acetylcholine-activated channels in mouse skeletal muscle. *Biophysical Journal* **49**, 361a.

WEILAND, G. & TAYLOR, P. (1979). Ligand specificity of state transitions in the cholinergic receptor: behaviour of agonists and antagonists. *Molecular Pharmacology* **15**, 197–212.